

Bucknell University

Bucknell Digital Commons

Honors Theses

Student Theses

Spring 2021

Impacts of Using Tubular Sections in Open Web Steel Joists

Hollis (Cas) L. Caswell V

Bucknell University, hlc008@bucknell.edu

Follow this and additional works at: https://digitalcommons.bucknell.edu/honors_theses



Part of the [Civil Engineering Commons](#), [Computational Engineering Commons](#), and the [Structural Engineering Commons](#)

Recommended Citation

Caswell, Hollis (Cas) L. V, "Impacts of Using Tubular Sections in Open Web Steel Joists" (2021). *Honors Theses*. 572.

https://digitalcommons.bucknell.edu/honors_theses/572

This Honors Thesis is brought to you for free and open access by the Student Theses at Bucknell Digital Commons. It has been accepted for inclusion in Honors Theses by an authorized administrator of Bucknell Digital Commons. For more information, please contact dcadmin@bucknell.edu.

IMPACTS OF USING TUBULAR SECTIONS IN OPEN WEB STEEL JOISTS

By

Hollis Leland Caswell V

A thesis

Presented to the Honors Council

For Honors in Civil and Environmental Engineering at Bucknell University

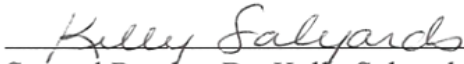
(Bachelor of Science in Civil and Environmental Engineering)

April 2021

Approved by



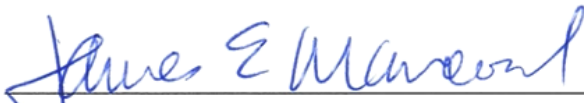
Advisor: Dr. Ronald D. Ziemian
Department of Civil and Environmental Engineering



Second Reader: Dr. Kelly Salyards
Department of Civil and Environmental Engineering



Department Chair: Dr. Stephen Buonopane
Department of Civil and Environmental Engineering



Honors Council Representative: Dr. James Maneval
Department of Chemical Engineering

ACKNOWLEDGEMENTS

I would first like to acknowledge my research advisor, Professor Ronald D. Ziemian, who inspired me to tackle this project and who provided ongoing guidance throughout the research. Professor Ziemian helped me understand the nuances of joist design and also set a standard of excellence that I will carry on long beyond my time at Bucknell University.

Next, I would like to thank Professor Kelly Salyards for supporting all of my work and providing some of the most useful advice over the past year to help me produce my best work without running out of steam.

Additionally, I would like to thank the entire Bucknell Engineering department for fostering an environment favoring primary research. The engaged, supportive team at Bucknell made this research possible and has helped direct my longer-term career aspirations.

I would also like to thank Scott Armbrust from Xbow for providing invaluable assistance by providing me with plans for the 32LTH06 tubular joist design that was instrumental to my research.

I would like to thank my good friend Eli Hiss for having such an interest in my study and continuously asking all sorts of questions that inspired me want to continuously look deeper my research.

Finally, I would like to thank both my parents, Lee Caswell and Melissa Baten Caswell, for their support and encouragement both throughout this research process, and throughout my entire education.

TABLE OF CONTENTS

ACKNOWLEDGEMENTS	i
TABLE OF CONTENTS	ii
LIST OF TABLES	v
LIST OF FIGURES	vi
ABSTRACT	ix
CHAPTER 1: INTRODUCTION.....	1
1.1 THESIS STATEMENT	1
1.2 OPEN WEB STEEL JOISTS	1
1.3 JOIST DESIGNS.....	4
1.3.1 ANGLES DESIGN.....	4
1.3.2 HSS DESIGN	6
1.3.3 HYBRID 1 DESIGN	7
1.3.4 HYBRID 2 DESIGN	8
1.4 MODELING OPEN WEB STEEL JOISTS.....	10
1.4.1 FINITE ELEMENT ANALYSIS	10
1.4.2 MASTAN2	10
1.4.3 STRAND7	11
1.5 PURPOSE AND OBJECTIVES	11
1.6 THESIS OVERVIEW	11
CHAPTER 2: BACKGROUND STUDIES	13
2.1 IMPACT OF USING TUBULAR CROSS-SECTIONS.....	13
2.1.1 LATERAL-TORSIONAL BUCKLING	13

2.1.2 JOIST CROSS-SECTIONAL PROPERTIES	15
2.1.3 ANTICIPATED RESULTS	16
2.2 MODEL COMPLEXITY	17
2.2.1 SINGLE DIMENSIONAL MODEL	18
2.2.2 LINE ELEMENT MODEL	19
2.2.3 MIXED ELEMENT MODEL	19
2.2.4 SHELL ELEMENT MODEL	21
2.2.5 PERCENT ERROR FOR EACH MODEL	22
CHAPTER 3: METHODOLOGY	24
3.1 TYPES OF ANALYSES	24
3.1.1 LBA – EIGENVALUE BUCKLING ANALYSIS	24
3.1.2 GNIA – IMPACT OF AN INITIAL IMPERFECTION	24
3.1.3 GMNIA – IMPACT OF INELASTIC MATERIAL PROPERTIES	25
3.2 LOAD CASES.....	26
3.2.1 POINT LOAD	26
3.2.2 DISTRIBUTED GRAVITY LOADS.....	27
3.2.3 UPLIFT.....	28
3.3 ACCOUNTING FOR SELF-WEIGHT	28
3.4 BRIDGING.....	28
CHAPTER 4: RESULTS	30
4.1 POINT LOAD RESULTS.....	30
4.2 DISTRIBUTED GRAVITY LOAD RESULTS	33
4.2.1 UNBRACED	33

4.2.2 MID-SPAN BRACED.....	37
4.2.3 QUARTER BRACED.....	41
4.2.4 IMPACT OF UNBRACED LENGTH.....	44
4.3 UPLIFT RESULTS	47
4.3.1 UNBRACED.....	47
4.3.2 MID-SPAN BRACED.....	47
4.3.3 QUARTER BRACED.....	48
4.3.4 IMPACT OF UNBRACED LENGTH.....	49
CHAPTER 5: CONCLUSIONS.....	50
5.1 SUMMARY OF RESULTS	50
5.2 FURTHER STUDIES	51
5.2.1 FURTHER ANALYSIS OF THE HYBRID 2 MODEL.....	51
5.2.2 INCREASE WEB STIFFNESS	51
REFERENCES.....	53
APPENDIX A: MODELS AND PROPERTIES.....	55
A-1 ANGLES DESIGN	55
A-2 HSS DESIGN.....	56
A-3 HYBRID 1 DESIGN.....	56
A-4 HYBRID 2 DESIGN.....	57
APPENDIX B: FINITE ELEMENT MODELS.....	58
B-1 LINE ELEMENT MODELS.....	58
B-2 MIXED ELEMENT MODELS.....	60
B-3 SHELL ELEMENT MODELS.....	61

LIST OF TABLES

Table 1. Comparison of each joist's cross-sectional properties	16
Table 2. Point Load – Impact of nonlinear and inelastic behavior.....	30
Table 3. Point Load – Impact of steel yielding	31
Table 4. Point Load – Impact of self-weight.....	32
Table 5. Unbraced Distributed Gravity Load – Impact of nonlinear and inelastic behavior	34
Table 6. Unbraced Distributed Gravity Load – Impact of steel yielding	34
Table 7. Unbraced Distributed Gravity Load – Impact of self-weight.....	36
Table 8. Mid-span Braced Distributed Gravity Load – Impact of nonlinear and inelastic behavior	37
Table 9. Mid-span Braced Distributed Gravity Load – Impact of steel yielding	38
Table 10. Mid-span Braced Distributed Gravity Load – Impact of self-weight.....	40
Table 11. Quarter Braced Distributed Gravity Load – Impact of nonlinear and inelastic behavior	42
Table 12. Quarter Braced Distributed Gravity Load – Impact of steel yielding	42
Table 13. Quarter Braced Distributed Gravity Load – Impact of self-weight.....	44
Table 14. Unbraced Uplift - Impact of self-weight	47
Table 15. Mid-span Braced Uplift - Impact of self-weight	48
Table 16. Quarter Braced Uplift - Impact of self-weight	48

LIST OF FIGURES

Figure 1. Open web steel joist system (SEAA, 2020).....	1
Figure 2. Lateral-torsional buckling on an open web steel joist.....	2
Figure 3. Lateral-torsional buckling with various levels of bridging.....	2
Figure 4. Joist geometry and terminology	3
Figure 5. Angle and HSS cross-sections	4
Figure 6. 3D rendering of the Angles joist.....	5
Figure 7. Angles joist cross-section design	5
Figure 8. 3D rendering of the HSS joist.....	6
Figure 9. HSS cross-section of chords	6
Figure 10. 3D rendering of the Hybrid 1 joist.....	7
Figure 11. Hybrid 1 cross-section of chords	7
Figure 12. 3D rendering of the Hybrid 2 joist.....	8
Figure 13. Hybrid 2 cross-section of chords	9
Figure 14. Shear-coupled forces induced by torsion	15
Figure 15. Anticipated joist capacities using Equation 1 for various unbraced lengths.....	17
Figure 16. Example of a single dimension model	19
Figure 17. Example of a line element model.....	19
Figure 18. Example of a mixed element model of the Angles design.....	20
Figure 19. Mixed element model connections	20
Figure 20. Example of a shell element model of the Angles design	21
Figure 21. Shell element model web connections	21
Figure 22. Angles LBA - Error of different models.....	22

Figure 23. HSS LBA - Error of different models	23
Figure 24. Hybrid 1 LBA - Error of different models	23
Figure 25. Initial lateral imperfections for various bracing.....	25
Figure 26. Erection of joist (Cole, 2018).....	27
Figure 27. Point loading	27
Figure 28. Distributed gravity loading	27
Figure 29. Uplift loading	28
Figure 30. Example of an FEM model with bridging (red arrows).....	29
Figure 31. Point Load – GNIA deflection	31
Figure 32. Point Load – GMNIA deflection	32
Figure 33. Point Load – GMNIA deflection including self-weight	33
Figure 34. Unbraced Distributed Gravity Load – GNIA deflection.....	35
Figure 35. Unbraced Distributed Gravity Load – GMNIA deflection	35
Figure 36. Unbraced Distributed Gravity Load – GMNIA deflection including self-weight	36
Figure 37. Mid-span Braced Distributed Gravity Load – GNIA deflection.....	39
Figure 38. Mid-span Braced Distributed Gravity Load – GMNIA deflection	39
Figure 39. Mid-span Braced Distributed Gravity Load – GMNIA deflection including self- weight	40
Figure 40. Web member yielding of the quarter braced Hybrid 2 under a gravity distributed load	41
Figure 41. Quarter Braced Distributed Gravity Load – GNIA deflection.....	43
Figure 42. Quarter Braced Distributed Gravity Load – GMNIA deflection	43
Figure 43. Quarter Braced Distributed Gravity Load – GMNIA deflection with self-weight	44

Figure 44. GMNIA capacities compared with anticipated results.....	45
Figure 45. GMNIA capacity as a function of unbraced length with self-weight	46
Figure 46. LBA uplift capacity as a function of unbraced length with self-weight	49
Figure 47. Defection of the joist cross-section	52
Figure 48. Geometric Properties of the Angles design (Schwarz, 2002)	55
Figure 49. Geometric Properties of the HSS design (Armbrust, 2020).....	56
Figure 50. Web member changes to the HSS design for the Hybrid 1 design	56
Figure 51. Chord member changes to the Angles design for the Hybrid 2 design.....	57
Figure 52. MASTAN2 line element model for the Angles design.....	58
Figure 53. MASTAN2 line element model for the HSS design.....	58
Figure 54. MASTAN2 line element model for the Hybrid 1 design.....	59
Figure 55. MASTAN2 line element model for the Hybrid 2 design.....	59
Figure 56. STRAND7 mixed element model for the Angles design.....	60
Figure 57. STRAND7 mixed element model for the HSS design.....	60
Figure 58. STRAND7 mixed element model for the Hybrid 1 design.....	60
Figure 59. STRAND7 shell element model for the Angles design	61
Figure 60. STRAND7 shell element model for the HSS design	61
Figure 61. STRAND7 shell element model for the Hybrid 1 design	61

ABSTRACT

Open web steel joists are lightweight structural trusses used in place of I-beams to support long-span floors and roofs of open space buildings. Their slender geometry makes them highly efficient in resisting flexure, but susceptible to out-of-plane buckling in a failure mode known as lateral-torsional buckling. This failure can be avoided by running lateral bracing between joists called bridging or potentially by using tubular sections to build up the joists rather than angle sections.

It is possible that a joist design using tubular cross-sections could require less bridging and prevent the need to use erection bridging for initial joist construction. Tubular sections provide good resistance to bending along with significantly higher resistance to torsion. While torsion resistance has little impact on capacity on small unbraced lengths, it has high impacts on large unbraced lengths.

This thesis examines the structural characteristics of a tubular design for a 32LH06 joist layout and the results suggest a change to the joist cross-section to increase the joist efficiency. The findings indicate that a tubular design can provide required torsional stability while improving safety for installers.

CHAPTER 1: INTRODUCTION

1.1 THESIS STATEMENT

Although open web steel joists are inherently susceptible to out-of-plane twisting and bending, moving from the use of angles to tubular sections in their chords substantially increases the strength of the joist while eliminating the need for bridging.

1.2 OPEN WEB STEEL JOISTS

Open web steel joists are slender lightweight structural trusses, as seen in red in Figure 1, that support floors and roofs of open space buildings, including manufacturing plants, airport hangars, warehouses, and supermarkets. As a system, these trusses are very strong and stiff and can be used in place of heavier and more expensive alternatives, such as I-beams. These joists are able to support large vertical loads, but require steel bridging connecting adjacent joists, shown in yellow in Figure 1.

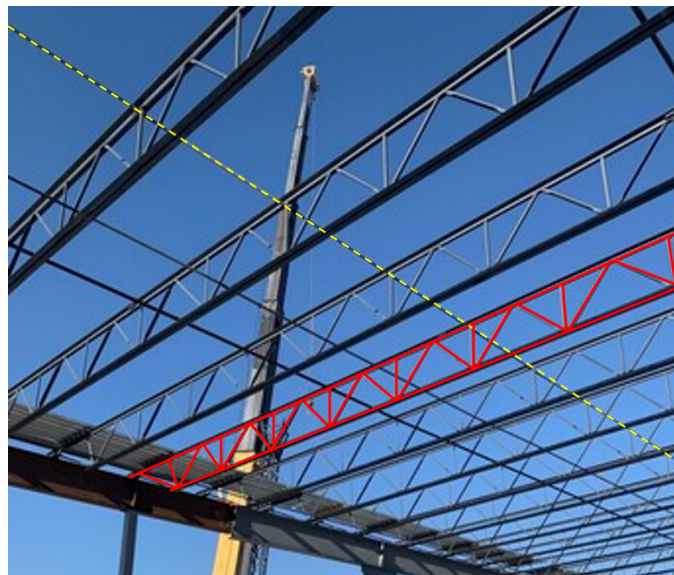


Figure 1. Open web steel joist system (SEAA, 2020)

Bridging connecting joists creates a full joist system and is important for preventing failure of any individual joist. Without bridging, joists are subject to twisting and buckling out of plane in a failure mode known as lateral-torsional buckling, shown in Figure 2.

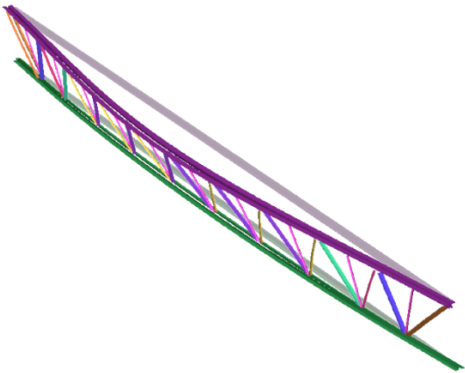


Figure 2. Lateral-torsional buckling on an open web steel joist

While other structural members besides joists are subject to lateral-torsional buckling, open web steel joists are designed for long spans with very slender cross-sections to make them economical which makes them especially susceptible to this failure mode. A joist’s resistance to lateral-torsional buckling depends on the largest unbraced length. It is therefore beneficial to brace the joist at locations such as the mid-span and quarter points as shown in Figure 3. Bridging between joists does not prevent lateral-torsional buckling, but rather forces them to fail at more complex buckling modes as shown in Figure 3 where higher loads are required to reach failure.

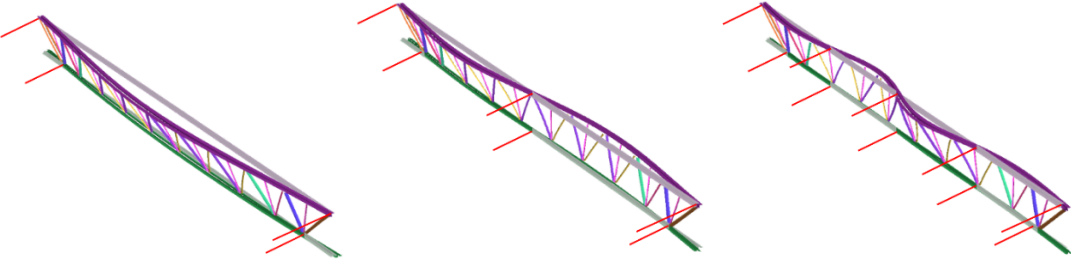


Figure 3. Lateral-torsional buckling with various levels of bridging

The complex truss geometry of these joists makes it difficult to use typical equations to predict their actual capacity, but the equations still can be used to predict how changes in the cross-section will impact their capacity.

The main structural part of the joists are the members on top and bottom of the truss. These members that span the trusses length are the chords of the truss, shown in pink in Figure 4. The members between the chords are known as web members and the connections of web members to chords are called panel points. Diagonal web members are important to both hold the chords together and transfer loads of the joist between the chords. The vertical web members are used to stiffen the top chord, which is typically the chord in compression, to resist buckling. As long as the web members themselves do not reach failure, they have little impact on the actual overall strength of the joists. As a large simplification, the truss can be considered to have no web members, but restrict the chords from deforming independently, essentially treating the chords together as a single beam. This simplification is used in this study to both choose chords for the joist designs studied and initially predict their capacities.

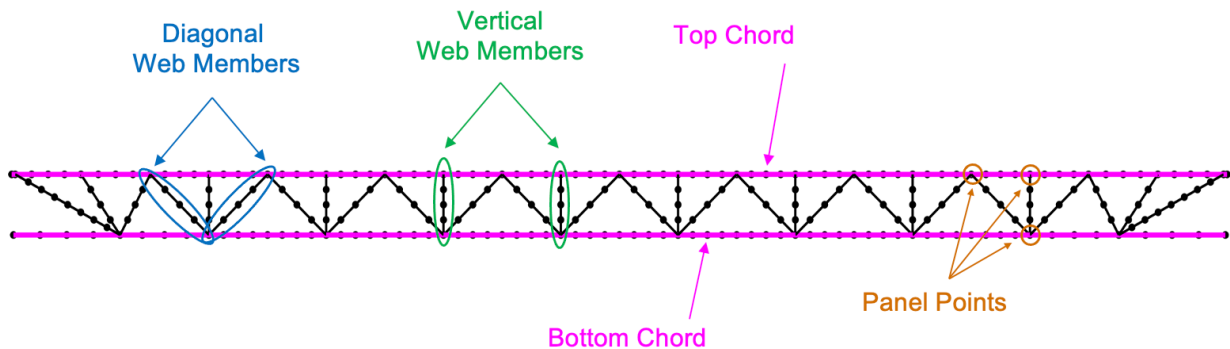


Figure 4. Joist geometry and terminology

1.3 JOIST DESIGNS

To compare the capacities of different cross sections, four unique joists were modeled. Each joist is 57 feet long and 32 inches deep based on 32LH06 joist design made up of angles. The 32LH06 joist uses a modified Warren Truss geometry with the addition of vertical web members bracing the top chord. The cross-sections of all chords and web members in each joist design is either made up of single and double angles or hollow structural steel sections known as HSS shown below in Figure 5 below. While the cost was not analyzed in this study, it should be noted that HSS sections are significantly more expensive than angles sections.

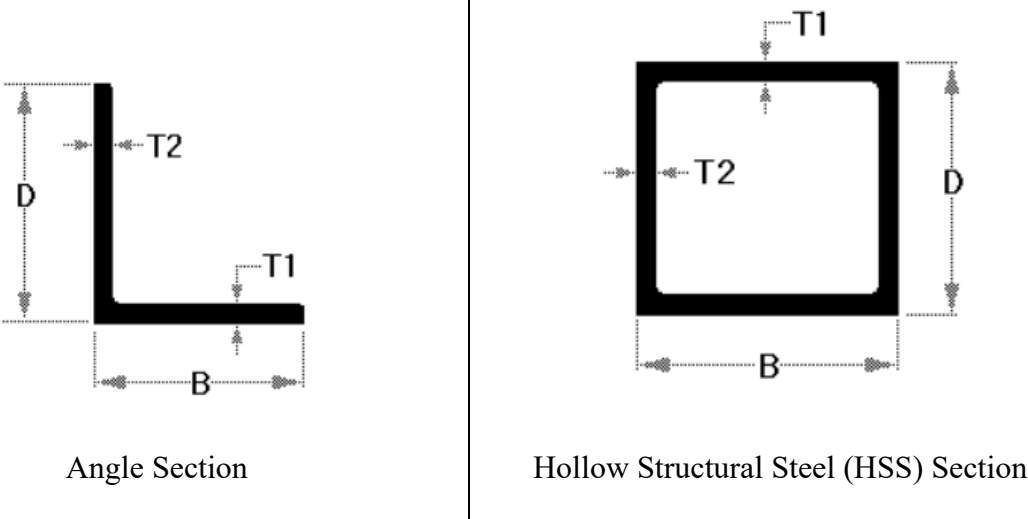


Figure 5. Angle and HSS cross-sections

1.3.1 ANGLES DESIGN

The joist shown in Figure 6, is a standard joist layout made up of angle and double angle sections used in practice and therefore will be used as the baseline in this study to compare with all other joists. This joist will be referred to as the Angles design from here on. The Angles joist design uses double angles for the chords as shown in Figure 7 with a combination of angles and double angles for the web sections. While all the web sections are made up of angles, most of the

angles in the web section are slightly different dimensions indicated with different colors in Figure 6. The web members made up of single angles attached to the chords by being crimped and welded in between the double angles that make up the chords. The end web members are double angles designed to take much higher loads than other web members because they transfer all the load from the bottom chord to the supports at the ends of the top chord. The double angle web members are attached to the legs of the double angles that make up the chord. The panel point spacing is uniform with exception of the last two panel points on the top chord that are spaced slightly further apart than the others. The specific dimensions for each section are provided in Appendix A-1.

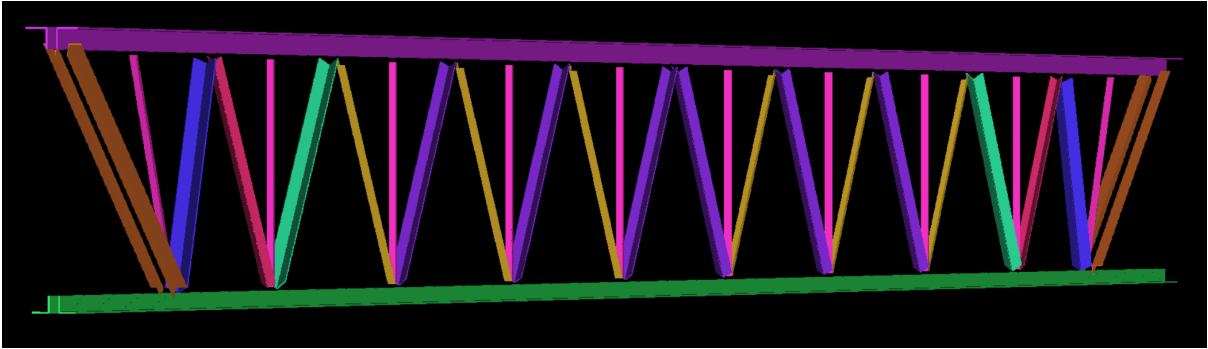


Figure 6. 3D rendering of the Angles joist

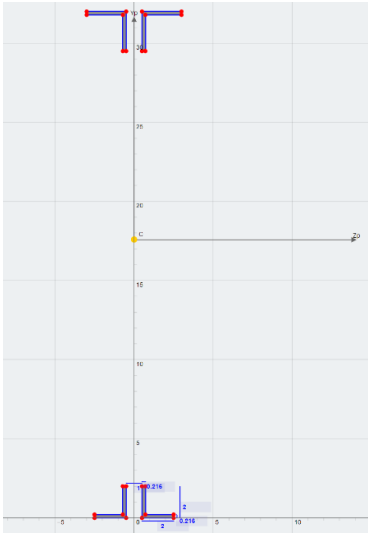


Figure 7. Angles joist cross-section design

1.3.2 HSS DESIGN

The HSS design (Armbrust, 2020) is made up of all HSS members for both the chords and web members as seen in Figure 8. The chords are single HSS members as seen in Figure 9 and therefore require the web members to be cut to the specific lengths and angles to allow for welded connections. While this design follows the basic geometry of the Angles joist, vertical web members are not included in this design. The number of diagonal web members remains the same as that of the angles. The dimensions of the web members are more consistent in this design. The panel point spacing is fully uniform in this design. Specific dimensions for each section are provided in Appendix A-2.

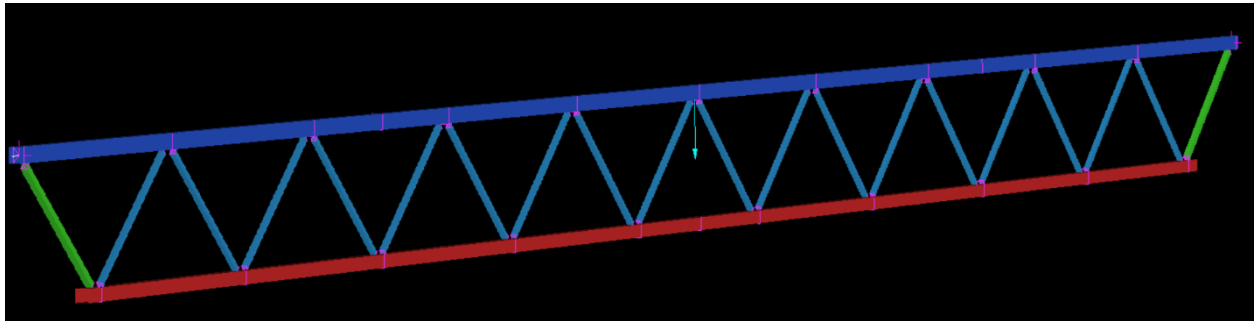


Figure 8. 3D rendering of the HSS joist

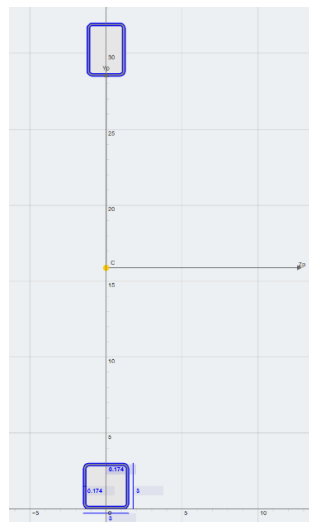


Figure 9. HSS cross-section of chords

1.3.3 HYBRID 1 DESIGN

The Hybrid 1 design uses a combination of HSS and angle sections as seen in Figure 10 with the intention of creating a more economical version of the HSS design that ideally provides the same capacity. The chords of the Hybrid design are the same chords used in the HSS design as seen in Figure 11. The difference in this design is the use of angle members for the web that are welded to the exterior of the chords by alternating sides. Unlike the HSS design, the web members do not need to be cut at specific angles which allows for easier assembly. The angles chosen for these web members were chosen such that their cross-sectional area match the cross-sectional area of the HSS web members.

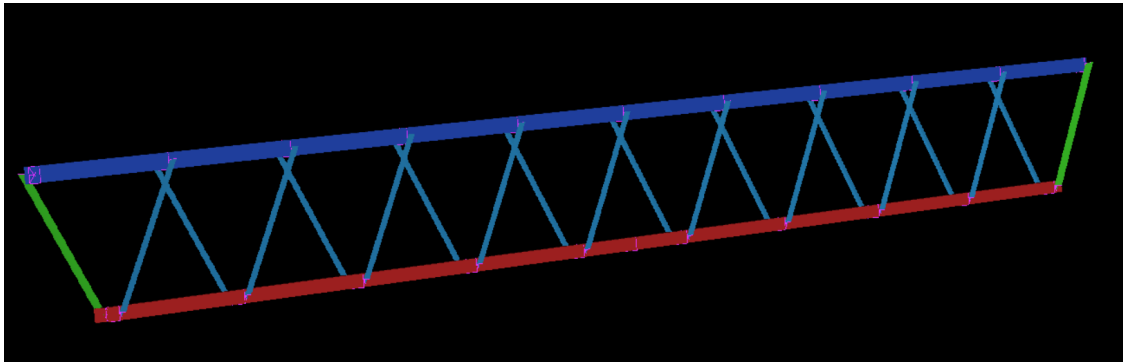


Figure 10. 3D rendering of the Hybrid 1 joist

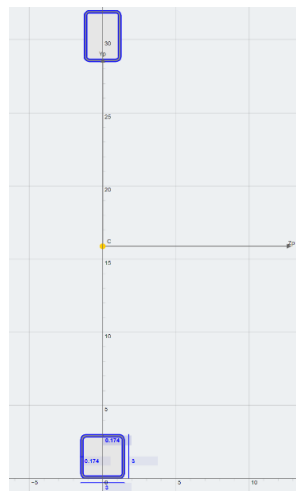


Figure 11. Hybrid 1 cross-section of chords

Specific dimensions for the Hybrid 1 layout and chord properties are the same as those in the HSS model, provided in Appendix A-2. The specific dimensions for each of web sections are provided in Appendix A-3.

1.3.4 HYBRID 2 DESIGN

The Hybrid 2 design was created to attempt to optimize the AISC lateral-torsional buckling equation by increasing the minor axis moment of inertia as well as the torsion constant. The Hybrid 2 is a less economical design than the Hybrid 1 because it uses four HSS members instead of two. This design uses the same layout and web members as the Angles design as seen in Figure 12, but modifies the double angles in the chords to double HSS sections shown in Figure 13. Specific dimensions for the joist layout and web member properties are the same as those in the Angles design provided in Appendix A-1. The specific dimensions for the chords are provided in Appendix A-4. This joist design was created further into this study than the other three joist designs and is therefore not considered in every analysis.

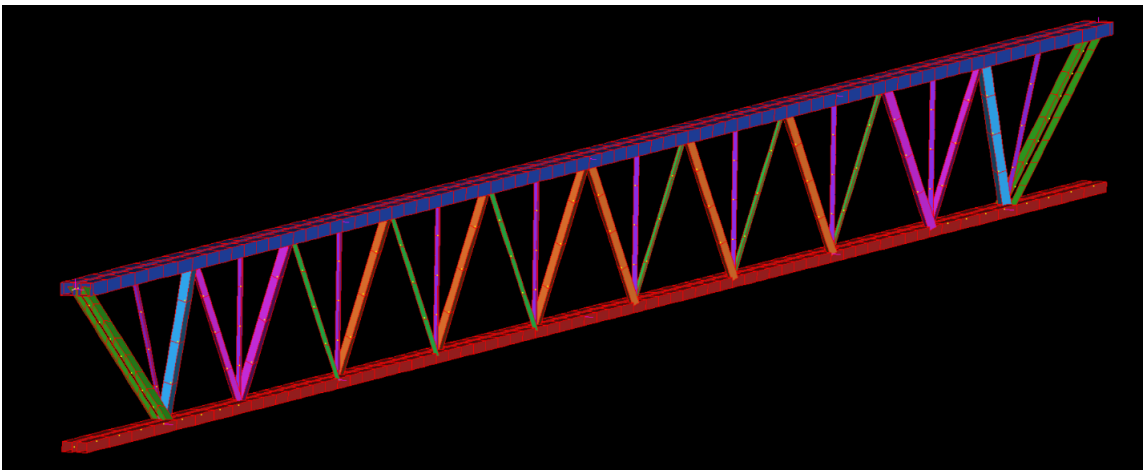


Figure 12. 3D rendering of the Hybrid 2 joist

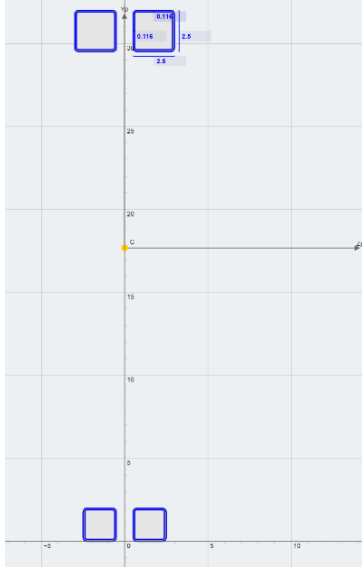


Figure 13. Hybrid 2 cross-section of chords

1.4 MODELING OPEN WEB STEEL JOISTS

1.4.1 FINITE ELEMENT ANALYSIS

Finite element analysis is a technique of modeling and analyzing systems by dividing the system up into smaller elements and treating each one as its own system. Each element can be solved on its own using the boundary conditions between elements to ensure compatibility of the stresses, loads, deflections, and deformations throughout the entire model. Depending on how the model is broken up, the number of equations needed to be solved changes. Each node has six degrees of freedom resulting in six equations to be solved. Each line element needs to be connected by a node at each end while each shell element requires a node at all four vertices of each shell. These powerful modeling methods are too time consuming to do by hand but can be easily solved by a computer. In this study, two finite element analysis programs, MASTAN2 and STRAND7, were used to analyze the various joists.

1.4.2 MASTAN2

MASTAN2 is a free educational finite element analysis program developed by Professor Ronald D. Ziemian that can model line elements in 3-dimensional space. The line elements are linked with both cross-sectional properties and material properties. While line elements are fairly accurate, there are still simplifications made to these models on a local level. Cross-sections given to a line element are not able to deform, meaning that local buckling or even general distortion across a member is neglected.

1.4.3 STRAND7

STRAND7 is a commercial finite element analysis program which has similar functionalities to MASTAN2 with regards to line element modeling, but also can be used for shell element modeling. Shell elements are given material properties similar to line elements, but the actual cross sections or each member are built up by shell elements which each have their own thickness allowing the cross-section to deform. Although this program can be more versatile, STRAND7 analyses take significantly more time to run the same analyses in MASTAN2. Both programs have the capability of running all the analyses used in this study.

1.5 PURPOSE AND OBJECTIVES

The purpose of this thesis is to determine how the use of tubular cross-sections in open web steel joists impacts their load capacity. The results will be presented to the Steel Joist Institute to suggest potentially more efficient steel sections for joist designs. The impact of these sections can be analyzed by creating finite element models of joist with various cross-section properties. Failure analyses of these designs under different types of loading and various levels of bridging will inform the most efficient joist design in regards to the amount of steel used.

1.6 THESIS OVERVIEW

The chapters of this thesis are organized in the following manner:

Chapter 1 contains the thesis statement, provides a background of open web steel joists, lateral-torsional buckling, Finite element analysis and the programs used for this study.

Chapter 2 provides the analysis of how the cross section impacts the lateral-torsional buckling capacity along with a linear buckling analysis study to determine the required model complexity.

Chapter 3 provides details of the types of loading cases tested along with the various types of analyses performed.

Chapter 4 discusses the results of all the loading types and their implications.

Chapter 5 provides suggestions for choosing more efficient joists and ways to further the efforts of this study.

Appendix A provides the section specifications for each of the joist designs.

Appendix B provides figures of the various finite element analysis models using different types of elements.

CHAPTER 2: BACKGROUND STUDIES

2.1 IMPACT OF USING TUBULAR CROSS-SECTIONS

Tubular cross-sections, such as rectangular HSS, are highly resistant to in-plane buckling and lateral-torsional buckling. These cross-sections exhibit high resistance to bending about their major and minor axes and demonstrates a high resistance to torsion. This is important because both bending and torsional resistance have an impact on the resistance of a cross-section to lateral torsional buckling.

2.1.1 LATERAL-TORSIONAL BUCKLING

Because of the complexity of the lateral-torsional buckling phenomenon, prediction of a member's critical moment capacity needs to incorporate aspects of both bending and torsion. The American institute of steel construction developed Equation 1 (AISC, 2016) to predict this critical capacity, and this equation gives us insight into how changes to the cross-section properties impact the joist capacity. While this equation is meant for I-shape members, it can be applied to open web steel joists, after making some assumptions, to determine the main factors affecting lateral-torsional buckling. Firstly, this equation assumes elastic lateral-torsional buckling is always occurring without any yielding or material inelastic behavior. This equation also assumes a uniform cross section along the length. For the purposes of estimating the joist capacities with this equation, the effects of the web members are assumed to be negligible, and the cross-section is assumed to be just the chord members. Additionally, this equation assumes that there are no deformations in the cross-section of the chords along the length. Finally, the equation assumes

doubly symmetric shapes and although the top and bottom chords of each joist are slightly different dimensions, the difference is assumed to be negligible for the purposes of this capacity estimation.

$$M_{cr} = C_b \frac{\pi}{L_b} \sqrt{EI_y GJ + \left(\frac{\pi E}{L_b}\right)^2 I_y C_w} \tag{Equation 1}$$

$$\text{Where } C_w = \frac{I_y h_0^2}{4}$$

- M_{cr} = Critical Moment Capacity (kip-in)
- C_b = Moment Adjustment factor
- L_b = Unbraced Length (in)
- E = Modulus of Elasticity (29,000 ksi)
- I_y = Moment of Inertia about the Minor axis (in⁴)
- G = Shear Modulus of Elasticity (11,200 ksi)
- J = Torsion Constant (in⁴)
- C_w = Warping Coefficient (in⁶)
- h_0 = Height between Flanges (in)

Although there are many different variables in Equation 1, only the torsion constant, J, moment of inertia about the minor axis, I_y, the height between the flanges, h₀, and the warping coefficient, C_w, are functions of the cross section. The torsion constant is how well twist can be resisted through coupled shear forces along its cross section. The torsion constant is significantly increased when looking at closed cross-sections compared to open cross-sections due to how the coupled shear forces caused by torsion are distributed relative to each other as shown in Figure 14. The moment

of inertia about the minor axis is how resistant a cross-section is to lateral bending. The moment of inertia about the minor axis is a function of how laterally spread out the cross-sectional area is. The warping constant is the resistance to warping in the flanges and is a function of minor axis moment of inertia and the height between flanges.

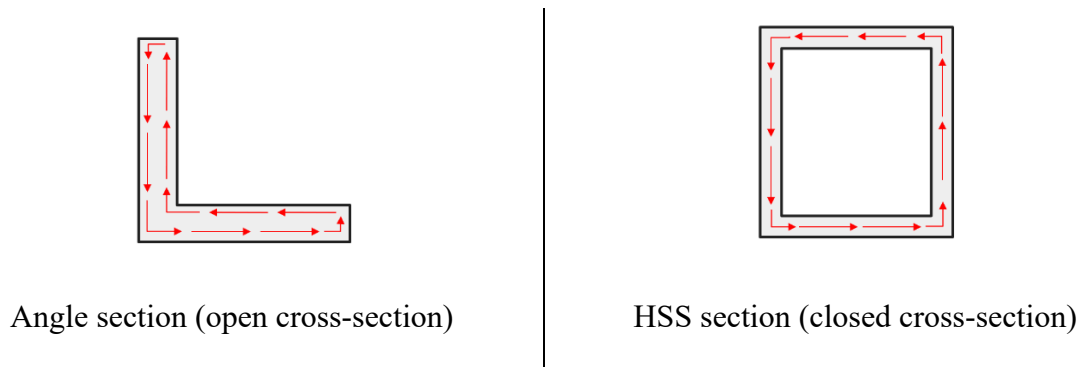


Figure 14. Shear-coupled forces induced by torsion

These cross-sectional properties effect the two terms under the radical shown in red and purple. The larger these two terms are, the larger buckling capacity the joist will have. It is important to recognize that the first term under the radical (in red) will only change if the cross-section changes while the second term (in purple) is both dependent on the cross-section and the unbraced length. For large unbraced lengths, the second term becomes negligible compared to the first term meaning that its capacity is controlled by the torsion constant and the minor axis moment of inertia. With small unbraced lengths, the buckling capacity is controlled by the second term under the radical which is dependent on the warping constant and the minor axis moment of inertia.

2.1.2 JOIST CROSS-SECTIONAL PROPERTIES

Using a section builder from SkyCiv and information about the joist layouts, the total self-weights and the cross-sectional properties of the chords of each joist were determined below in Table 1. Although self-weight and cross-sectional area are not considered in Equation 1, it was

important to ensure that the models being compared had approximately the same amount of steel overall and in the chords to ensure that the capacity results were truly a reflection of changes to the joist cross-sectional geometries.

Table 1. Comparison of each joist’s cross-sectional properties

(Values in parentheses are property values as a ratio of the Angles design value for the same property)

	Angles	HSS	Hybrid 1	Hybrid 2
Self-Weight (lbs)	836 (1.00)	861 (1.03)	828 (0.99)	894 (1.07)
Cross-Sectional Area (in)	3.66 (1.00)	3.76 (1.03)	3.76 (1.03)	3.81 (1.04)
Moment of Inertia, I_y (in⁴)	6.68 (1.00)	4.26 (0.64)	4.26 (0.64)	13.26 (1.99)
Height Between Flanges, h_o (in)	30.72 (1.00)	28.75 (0.94)	28.75 (0.94)	29.75 (0.97)
Torsion Constant, J (in⁴)	0.05 (1.00)	7.84 (156)	7.84 (156)	4.76 (95)
Warping Constant, C_w (in⁶)	1575 (1.00)	880 (0.56)	880 (0.56)	2934 (1.86)

The HSS and Hybrid 1 have the same chords, so it is anticipated that their capacities will be identical. The HSS and Hybrid 1 designs have a minor axis moment of inertia and warping constant of almost half that of the Angles design. On the other hand, the HSS and Hybrid 1 designs have a torsion constant 156 times larger than the Angles design. Although the HSS and Hybrid 1 torsion constants are much higher than the Angles torsion constant, the lower moment of inertia and lower warping constant suggests that there will be a critical unbraced length at which the Angles design will outperform the HSS design. Ideally that critical unbraced length is small enough where it will not be practical to actually brace the joist at that length.

The Hybrid 2 design was chosen based on this equation with the goal of maintaining the same weight and cross-sectional area, while maximizing the warping constant, torsion constant and the minor axis moment of inertia.

2.1.3 ANTICIPATED RESULTS

Using Equation 1 and the relationship between an applied distributed gravity load and moment (AISC, 2016, Table 3-23.1), the estimated joist capacities were determined below in Figure 15 for the unbraced joist configuration along with the half and quarter braced conditions. Based on the estimated capacities, the unbraced length appears large enough to expect that the HSS and Hybrid 1 will outperform the Angles in every reasonable bracing configuration. The Hybrid 2 is also predicted to have a capacity around 50% larger than the HSS and Hybrid 1 designs (slightly varying depending on the amount of bridging). This prediction suggests that the HSS and Hybrid models will be able to outperform the mid-span braced Angles model, but not the quarter braced capacity. It is important to note that these capacities do not take into account any yielding.

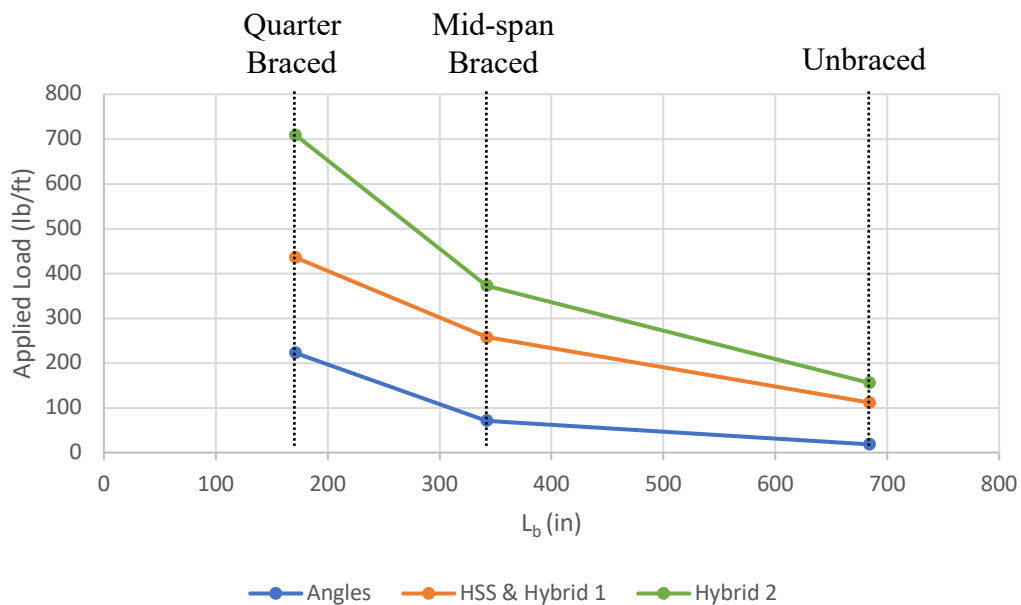


Figure 15. Anticipated joist capacities using Equation 1 for various unbraced lengths

2.2 MODEL COMPLEXITY

Finite Element Analysis results are as accurate as the models used to model them. Just because models can be very detailed does not mean that the models should take into account every detail

being modeled. The more complex the model, the longer it takes for the computer to run each analysis on the model. To be able to run sufficient studies on the joists, four levels of complexity were considered and compared to determine the simplest model that provides sufficiently accurate data. A linear Eigenvalue buckling analysis was performed without the influence of self-weight to compare all the models to each other. For the purposes of the comparison, the shell model buckling values were used as the most accurate buckling load values because of its higher level of detail. The Hybrid 2 design was added after this comparison was performed and was therefore not included in this background study.

2.2.1 SINGLE DIMENSIONAL MODEL

The single dimensional model, shown in Figure 16, represents the joist under the same assumptions as Equation 1. This model is made of line elements given the cross-section properties of the top and bottom chords together. This model assumes a uniform cross-section along the whole length of the joist by neglecting the impact of web members and assumes the top and bottom chords remain exactly in the same place relative to each other at any location along the length no matter how the overall joist deflects under loading. Because the web members are not considered, the HSS and Hybrid 1 models are identical for this model as they share the same members for their chords. Each element in this model has warping continuous properties turned on to allow the warping to be transferred along the length of the joist shown with light blue at each node in Figure 16.

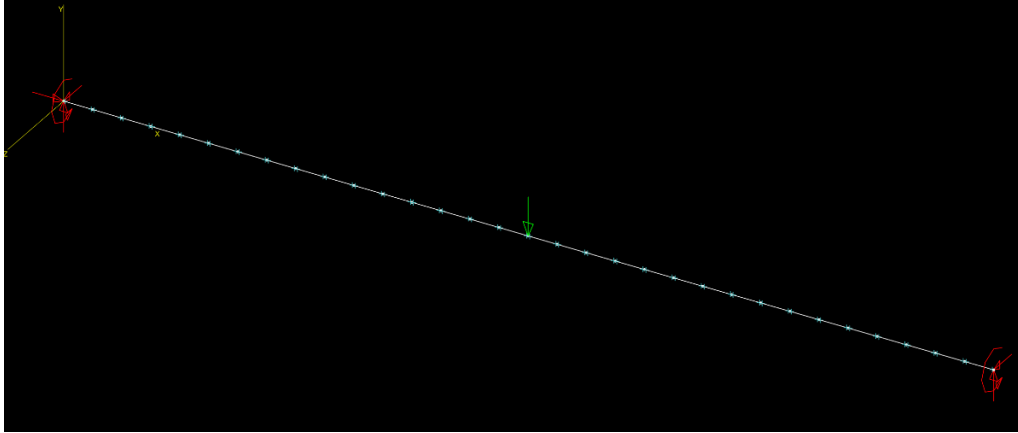


Figure 16. Example of a single dimension model

2.2.2 LINE ELEMENT MODEL

The line element model, shown in Figure 17, uses independent line elements for each web and chord member with the exception of double angles that were modeled together. The Hybrid 1 model included unique line elements acting like panel point connections with increased stiffness and no density to take into account the offsets of the web members.

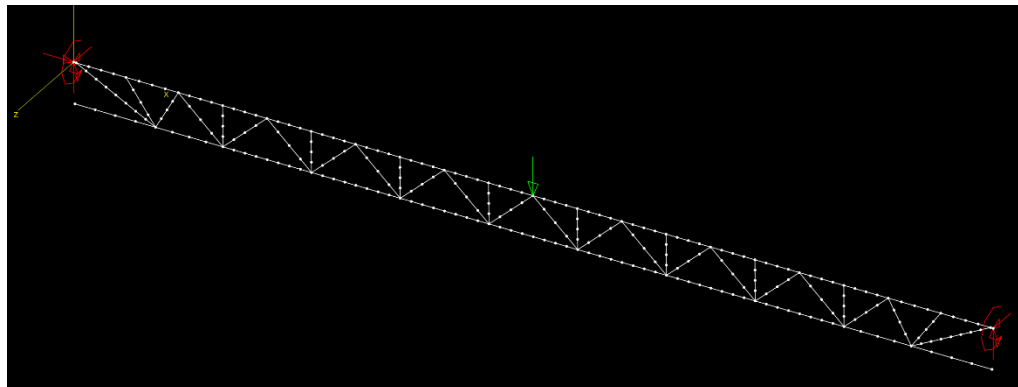


Figure 17. Example of a line element model

2.2.3 MIXED ELEMENT MODEL

The Mixed Element model, shown below in Figure 18, uses shell elements in the chords and line elements in the web members. This model assumes that although the web members do not

affect the results significantly and can be modeled as line elements whereas the chords have a large impact on the capacity and should be modeled as shell elements. To connect the line elements that made up the web to the shell elements that made up the chords at the panel points, stiff line elements were used. The stiff elements run along the free edges of the plate at the connection and then connected to a node at the centroid of the member which was then attached to the web line elements, as shown at the end of the joist in Figure 18 of isolated in Figure 19. These stiff connections were given different material properties including no density and a modulus of elasticity ten times larger than that of steel. Applied loads were placed at nodes placed at the centroids of the shell member panel point connections.

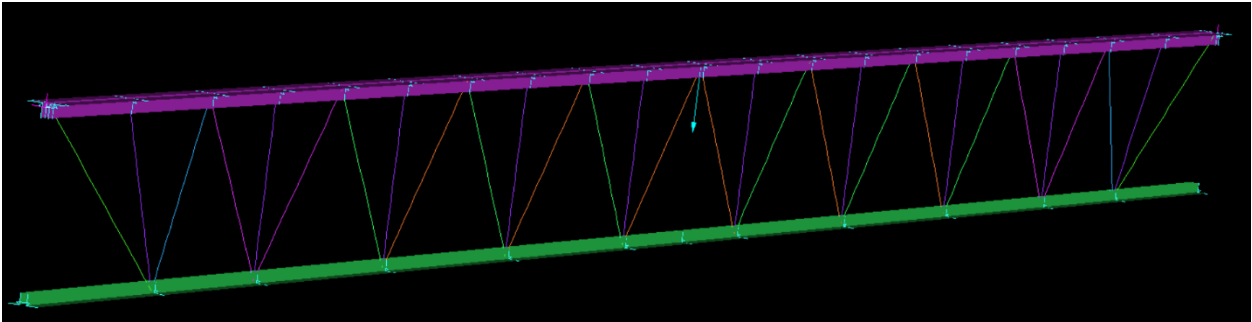
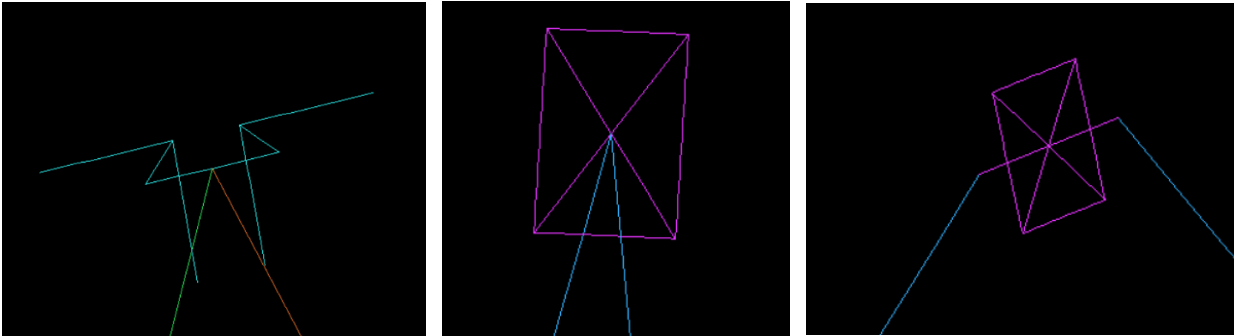


Figure 18. Example of a mixed element model of the Angles design



Angles Connection

HSS Connection

Hybrid 1 Connection

Figure 19. Mixed element model connections

2.2.4 SHELL ELEMENT MODEL

The shell model was the most detailed model used. All chord and web members were built up with shell members as seen in Figure 20. Although this model was made up of shells, the connections were made using stiff line elements connecting the ends of the members at points as seen in Figure 21. Loads were all applied at nodes placed at the centroids of the shell member in the same way as the mixed element models.

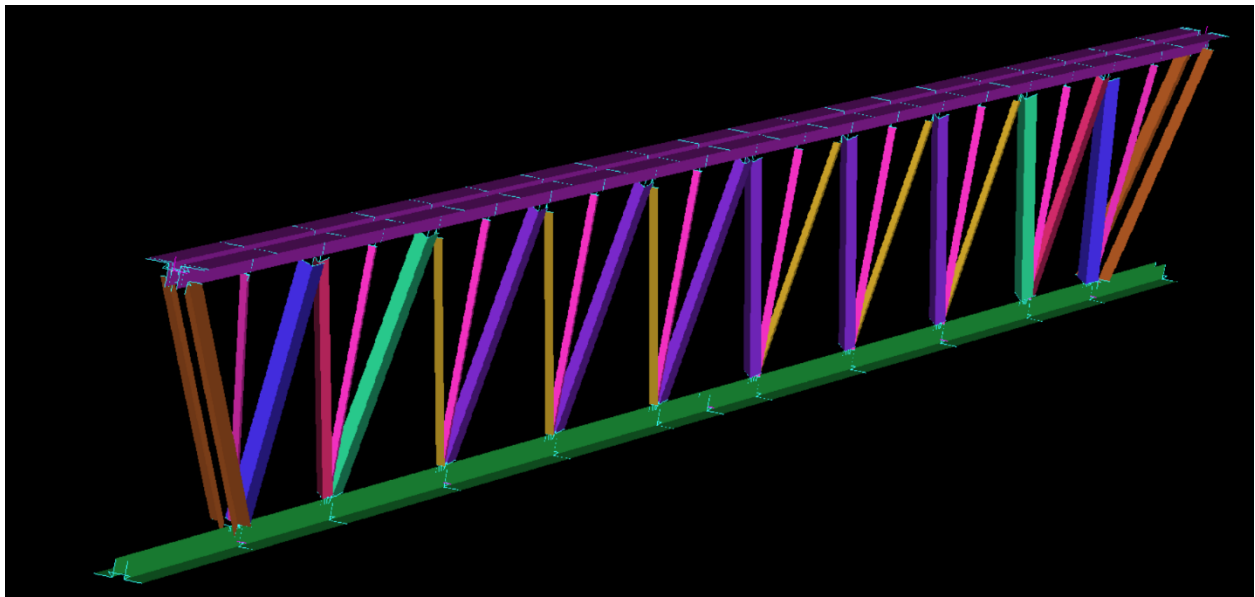
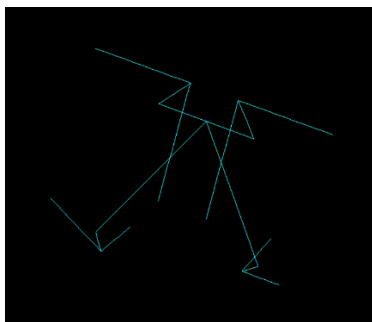
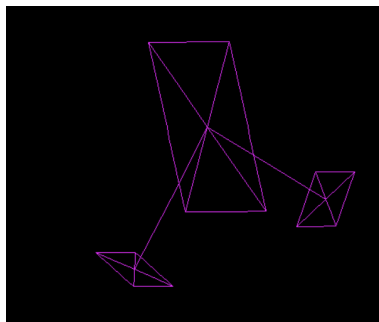


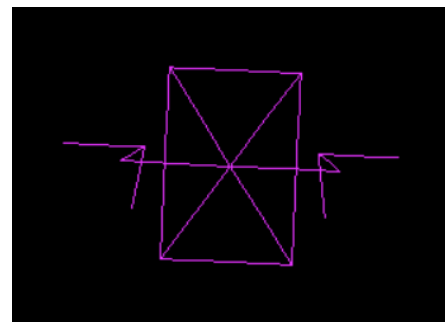
Figure 20. Example of a shell element model of the Angles design



Angles Connection



HSS Connection



Hybrid 1 Connection

Figure 21. Shell element model web connections

2.2.5 PERCENT ERROR FOR EACH MODEL

Each of the joist designs, with the exception of the Hybrid 2, was compared in the unbraced, mid-span braced and quarter braced conditions for each model complexity. As seen in Figures 22, 23, and 24, the single dimension model and Equation 1 had significant error compared to the other models of each design. The MASTAN2 line element models were determined to be sufficiently accurate based on this study. While the Angles model shows more error in the line element models compared to the other designs, the increase in time required to run the mixed element model was determined to be not worth the extra accuracy as it would not allow for enough time to run all the analyses that ended up being performed for this study. Line element models were therefore used

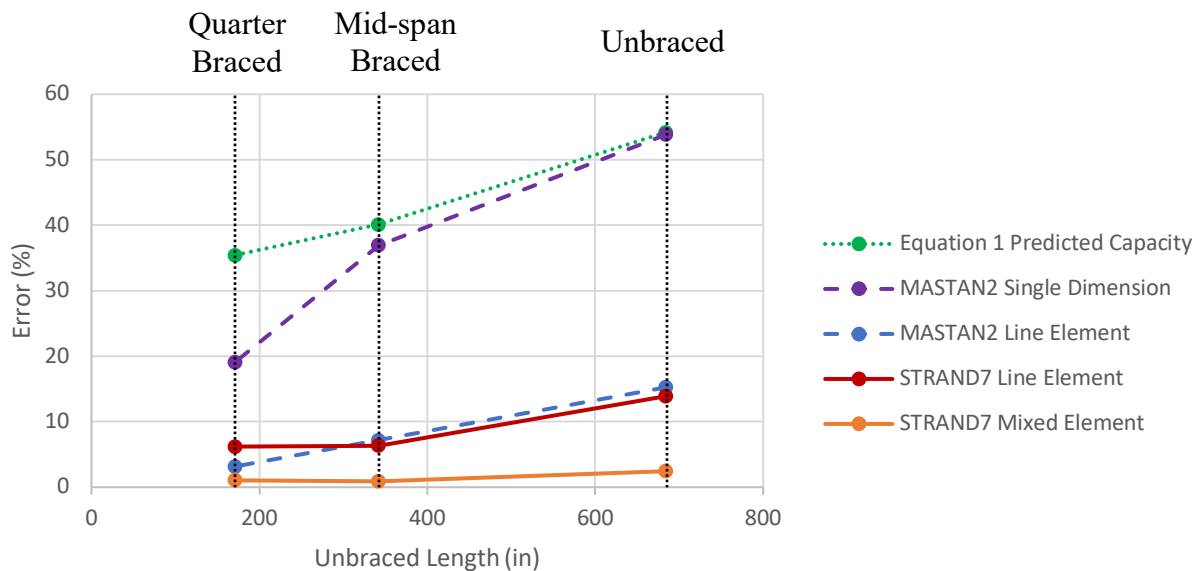


Figure 22. Angles LBA - Error of different models

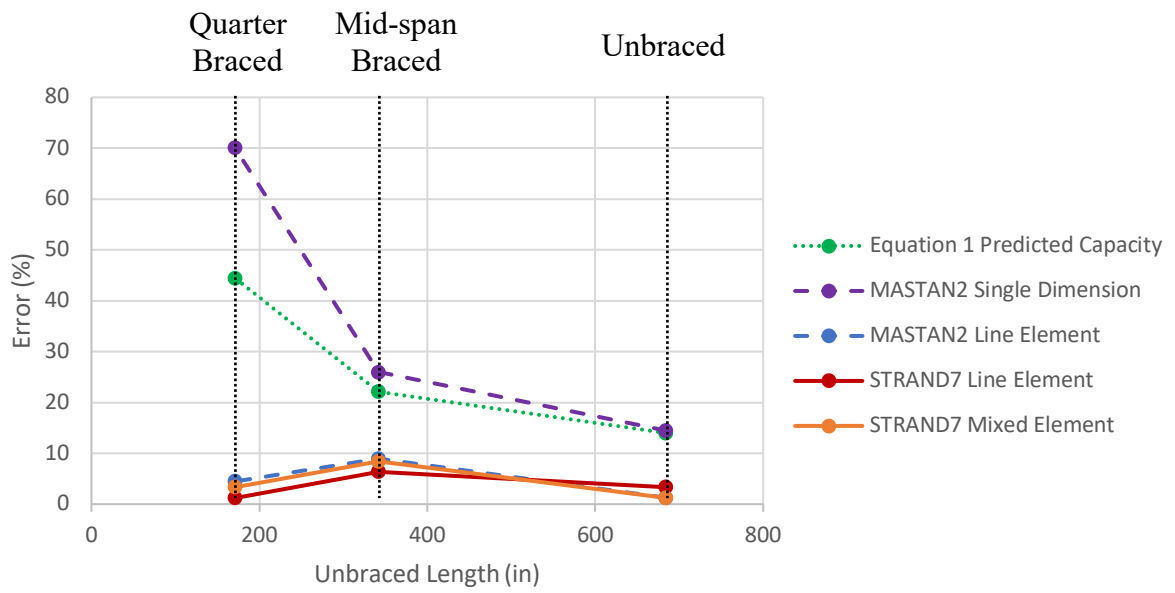


Figure 23. HSS LBA - Error of different models

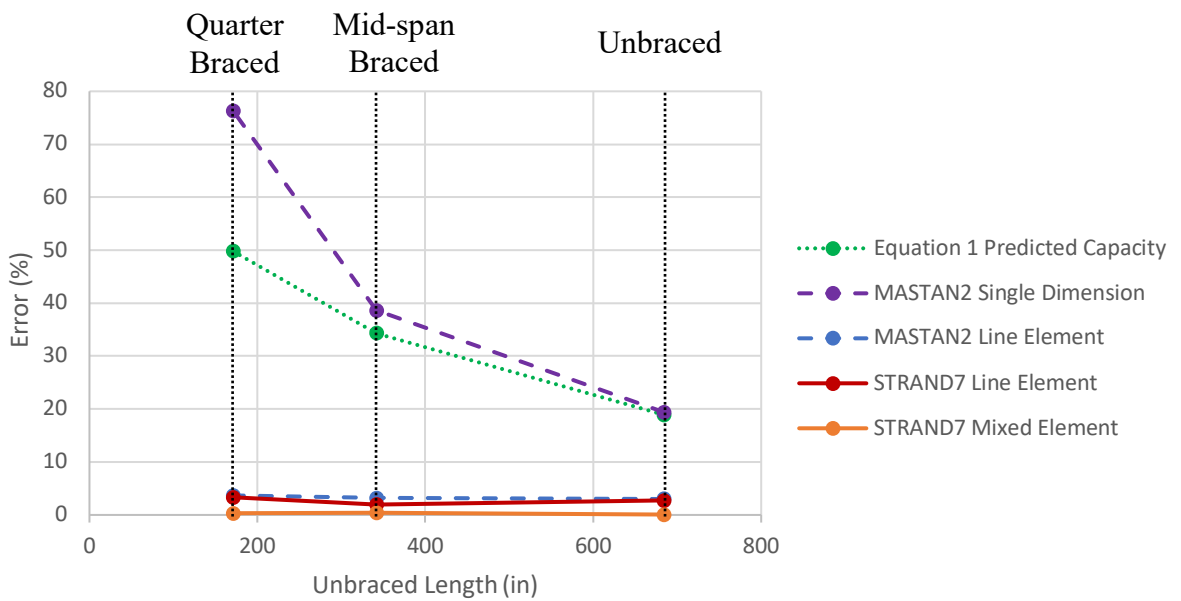


Figure 24. Hybrid 1 LBA - Error of different models

CHAPTER 3: METHODOLOGY

As discussed in Chapter 1, finite element models were used to analyze the various joists. After the background comparative study of the lateral buckling analyses, line models were determined to be sufficiently accurate for all further analysis.

3.1 TYPES OF ANALYSES

Three types of analysis were used for the finite element models. For all load cases, a linear buckling analysis (LBA) was performed. With only the exception of the uplift load case, a geometrical nonlinear inelastic analysis (GNIA) and a geometric and material nonlinear inelastic analysis (GMNIA) were also performed. All analyses were run with and without weight.

3.1.1 LBA – EIGENVALUE BUCKLING ANALYSIS

A linear buckling analysis, known as an LBA, assumes perfectly elastic behavior of all members. This means that as they are loaded, the deformation per unit of load is linear and the material does not yield. This analysis is solved using eigenvalues and provides a good estimate of the critical load and buckled conditions, but does not account for inelastic behavior or differentiate the direction that the joist will buckle. While this analysis is not as accurate as more sophisticated analyses that consider geometric and material inelastic behavior, it is much faster to run and can provide an upper bound limit of the actual capacities.

3.1.2 GNIA – IMPACT OF AN INITIAL IMPERFECTION

To look at the impact of an initial imperfection on the joist buckling capacities, a geometrical nonlinear inelastic analysis known as a GNIA was utilized. This analysis, unlike the LBA increases

loads incrementally and looks at records the joist deflection as a function of the increasing load. To perform this analysis the model needs to include an initial imperfection. To create the imperfection, an LBA is performed and then the model geometry can be updated as a scaled version of the LBA deflected shape. The updated geometries follow the specified imperfections shown in Figure 25.

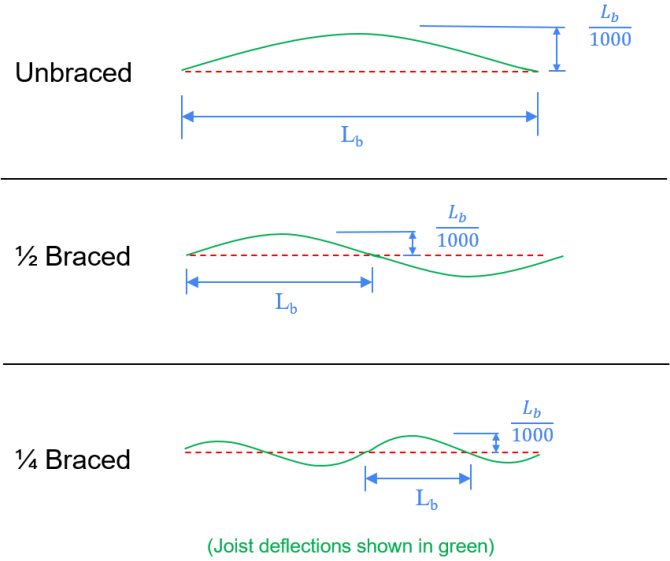


Figure 25. Initial lateral imperfections for various bracing

This analysis is elastic so there is not a clear capacity based on the results, but the lateral deflections of the joist will begin to deform at a nonlinear rate as it undergoes lateral-torsional buckling. For the purposes of this study, a limit state was chosen for this analysis when the incremental increase in load divide by the incremental deflection is less than six percent of the initial increase in load divided by the initial deflection.

3.1.3 GMNIA – IMPACT OF INELASTIC MATERIAL PROPERTIES

A geometrical and material nonlinear inelastic analysis known as a GMNIA was utilized to look at the impact of material yielding on the joist buckling capacities. This analysis takes into

account the inelastic material stiffness in addition to the initial imperfection in the joist that GNIA considers. The same limit state that is used for the GNIA will be used for the GMNIA so that the GMNIA and GNIA results can be compared to determine the impact of material yielding for each joist. Unlike the GNIA, this analysis has a clear point of failure as a result of the material yielding. The failure capacity can be compared to the LBA results to determine the impact of both material and geometric inelasticity combined.

3.2 LOAD CASES

Three different load cases were analyzed to represent the main ways the truss will be loaded over its lifespan. These loading cases include a point load representing initial joist erection, distributed gravity loading representing deck loads transferred to the joist along its length and uplift for roof decks. All three of these load cases were analyzed with and without self-weight.

3.2.1 POINT LOAD

The point load case was chosen to represent the type of loading a joist will initially undergo during initial joist erection. Open web steel joists are so slender that they need to be lifted by a crane attached only at the midpoint point to ensure they will not buckle during erection under their own self-weight. When joists are first placed on a structure, a construction worker must detach the joist from the crane erecting it as seen in Figure 26. Additionally, this loading case assumes that there is no bridging between adjacent joists yet. Figure 26 shows tabs on the joist where bridging will be attached between the joist with the construction worker and the adjacent joist, circled in red. This loading case will assume the construction worker is at the middle of the joist with all their weight on the top chord as shown in Figure 27.



Figure 26. Erection of joist (Cole, 2018)

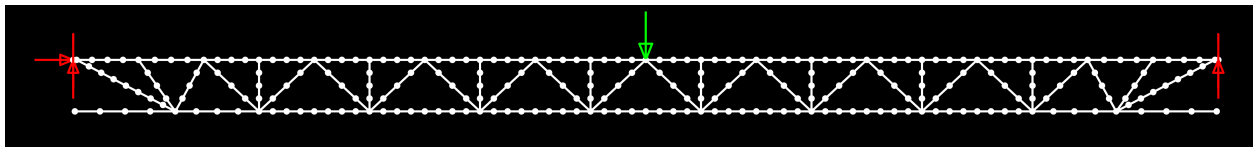


Figure 27. Point loading

3.2.2 DISTRIBUTED GRAVITY LOADS

The distributed gravity load case represents the loading after construction with the distributed gravity load representing appropriate dead and live loads transferred through the deck and applied to the truss. To avoid impacts of the inclusion of vertical web members on certain designs, the distributed gravity load was applied at the diagonal web panel points as shown in Figure 28 rather than along the entire top chord.

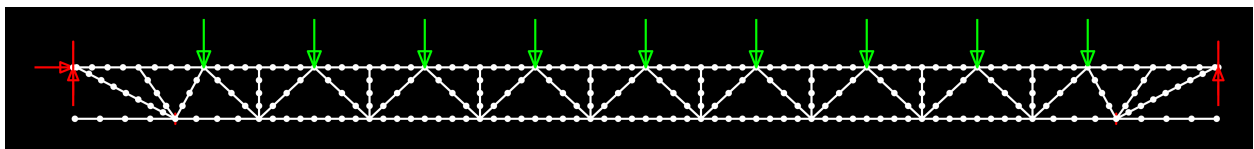


Figure 28. Distributed gravity loading

3.2.3 UPLIFT

This load case is the same as the distributed gravity load case, but with loads pushing upward at the same connections on the top chord as seen in Figure 29. Due to time constraints, only a linear buckling analysis was performed for uplift. For uplift loading, the bottom chord is put into compression and is the main part of the truss undergoing buckling. Lateral bracing in the bottom chord at the ends is essential to resist the bottom chord from buckling out of plane.

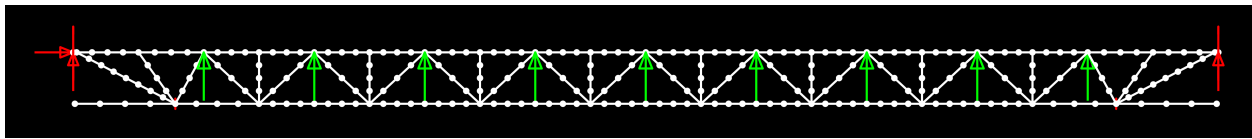


Figure 29. Uplift loading

3.3 ACCOUNTING FOR SELF-WEIGHT

Self-weight adds an additional level of complexity to running any of these analyses. Every analysis provides applied load ratios which can be scaled to find the capacity without self-weight, but cannot be done with self-weight. Both MASTAN2 and STRAND7 treat the density of a material as another load and therefore the applied load ratio is also the scaled self-weight. To accurately determine the capacity when incorporating self-weight, the loads have to be iteratively adjusted until failure occurs at an applied load ratio of one. For simplicity, only LBAs and GMNIAs were performed so that there would be no need to iteratively adjust the analyses until the limit state capacity defined in Chapter 3.1.2 occurred at an applied load ratio of one.

3.4 BRIDGING

To incorporate bridging into the models, fixities were placed at the panel points shown by the red arrows in Figure 30 restricting the lateral movement of the joist at the quarter points. Although

the bridging on the bottom edges of the joist, shown in red, are in place for uplift, they are in place for all distributed gravity load cases because the distributed gravity load cases represent the joist condition after construction with all bridging in place.

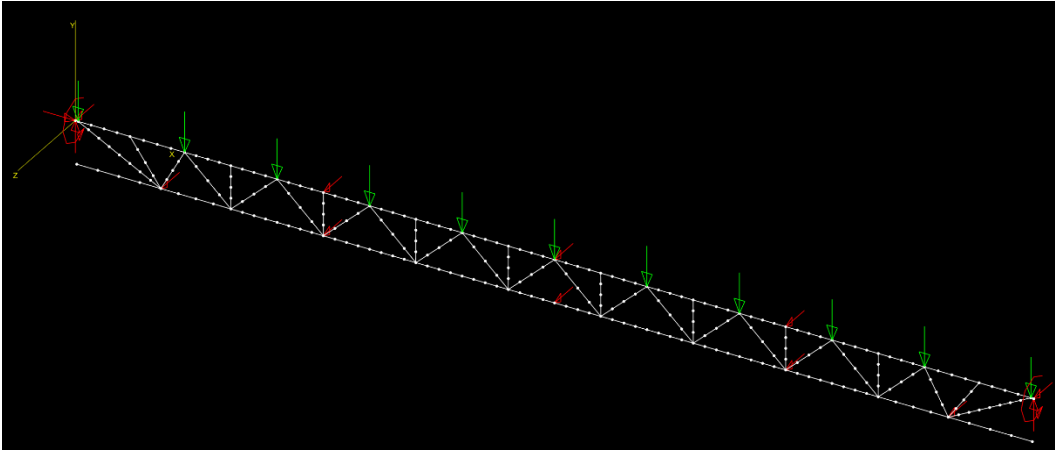


Figure 30. Example of an FEM model with bridging (red arrows)

CHAPTER 4: RESULTS

After running a LBA, a GNIA, and a GMNIA under the various load cases, both the capacities and the factors impacting joist capacity can be better understood. As stated in Chapter 3, the GNIA does not have a clear point of failure and is therefore difficult to compare to a point of failure, while the LBA has a point of failure as the only data point. For that reason, the LBA results are compared to the GMNIA failure point results while the GNIA limit state result will be compared with the GMNIA limit state result.

4.1 POINT LOAD RESULTS

Table 2 shows a consistent trend with the joist capacities with both the LBA and GMNIA results. Both analyses show the Angles design with the lowest capacity followed by the Hybrid 1 just below the HSS design, both with over two and a half times the capacity of the Angles design. The Hybrid 2 design has the highest capacity of just over four and a quarter times the capacity of the Angles design. The larger decrease in the Angles design capacity compared to the HSS and Hybrid 1 decreases explains why the GMNIA capacity load ratios of the HSS and Hybrid 1 joists are higher than the LBA capacity load ratios.

Table 2. Point Load – Impact of nonlinear and inelastic behavior

	Failure Load in kips (Angles Capacity Load Ratio)							
	Angles		HSS		Hybrid 1		Hybrid 2	
LBA	1.10	(1.00)	2.90	(2.63)	2.79	(2.53)	4.74	(4.29)
GMNIA	1.00	(1.00)	2.75	(2.74)	2.60	(2.59)	4.31	(4.30)
Capacity Decrease	9%		5%		7%		9%	

Although the GMNIA accounts for material yielding, Table 3 shows that there is no decrease in capacity when running a GMNIA compared to a GNIA for all joist designs under a point load.

This means that the decrease in capacities of the GMNIA from the LBA are solely a result of the initial imperfection. Under this unbraced loading case, the joists are long and slender enough that they undergo pure elastic lateral-torsional buckling before yielding ever occurs. The capacities of these joists are based purely on the cross-sectional geometry of the joists. The perfectly elastic behavior can be confirmed by noting that the GMNIA load deflection curves in Figure 32 have the same limit state deflection as the GNIA deflection curves in Figure 31 up to the limit state .

Table 3. Point Load – Impact of steel yielding

	Limit State Load in kips (Angles Capacity Load Ratio)			
	Angles	HSS	Hybrid 1	Hybrid 2
GNIA	0.80 (1.00)	2.25 (2.81)	2.20 (2.75)	3.80 (4.75)
GMNIA	0.80 (1.00)	2.25 (2.81)	2.20 (2.75)	3.80 (4.75)
Capacity Decrease	0%	0%	0%	0%

Although the buckling happens at different capacities, all four designs have relatively similar stiffness resulting in limit state capacities at approximately the same deflection as seen in Figure 31 and Figure 32.

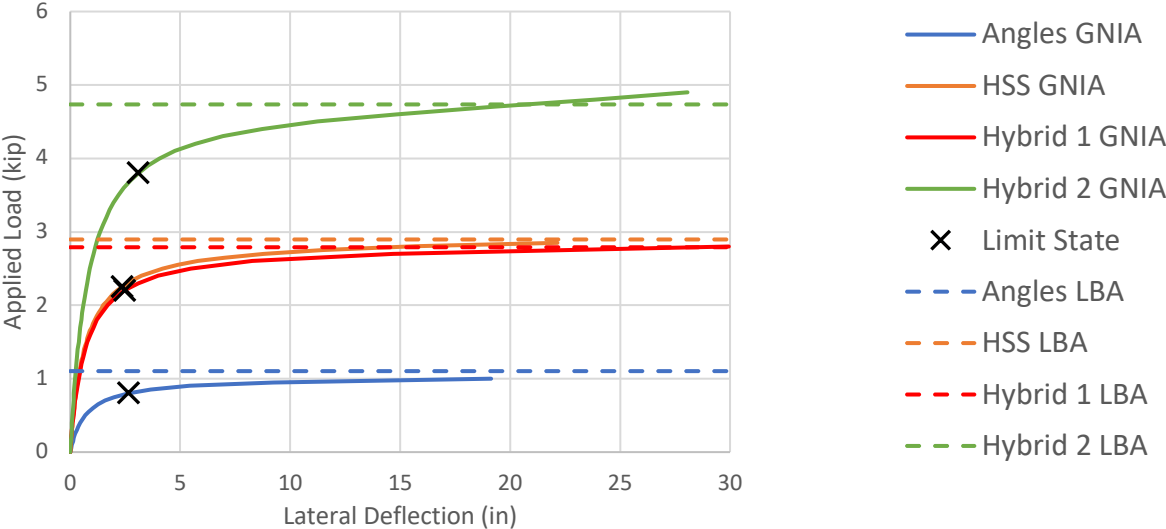


Figure 31. Point Load – GNIA deflection

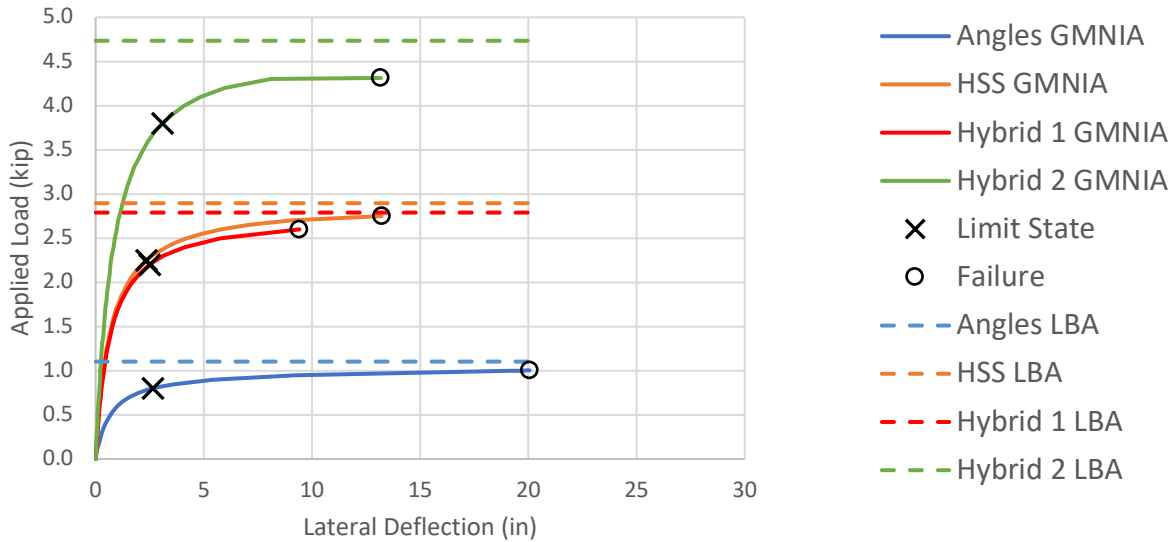


Figure 32. Point Load – GMNIA deflection

The inclusion of self-weight effects reduces each joist capacity by approximately the same amount because all designs have similar weights. The consistent capacity impact from self-weight impacts lower capacity joists more because the self-weight is a larger percentage of the total joist capacity. The Angles design has a decrease of over forty percent of its capacity when considering self-weight. Self-weight has only a seventeen percent impact on the HSS and Hybrid 1 designs and an even lower impact of 10 percent on the Hybrid 2 designs capacity.

Table 4. Point Load – Impact of self-weight

	GMNIA Failure Load in kips (Angles Capacity Load Ratio)							
	Angles		HSS		Hybrid 1		Hybrid 2	
Neglecting Self-Weight	1.00	(1.00)	2.75	(2.74)	2.60	(2.59)	4.31	(4.30)
Including Self-Weight	0.57	(1.00)	2.28	(4.00)	2.15	(3.78)	3.88	(6.82)
Capacity Decrease	43%		17%		17%		10%	

The deflections at failure of these models are also impacted by the inclusion of self-weight as seen in Figure 33. The Angles model has more than a twenty five percent reduction in lateral

deflection than before adding self-weight. All other designs have an almost negligible decrease in deflection at failure after adding self-weight.

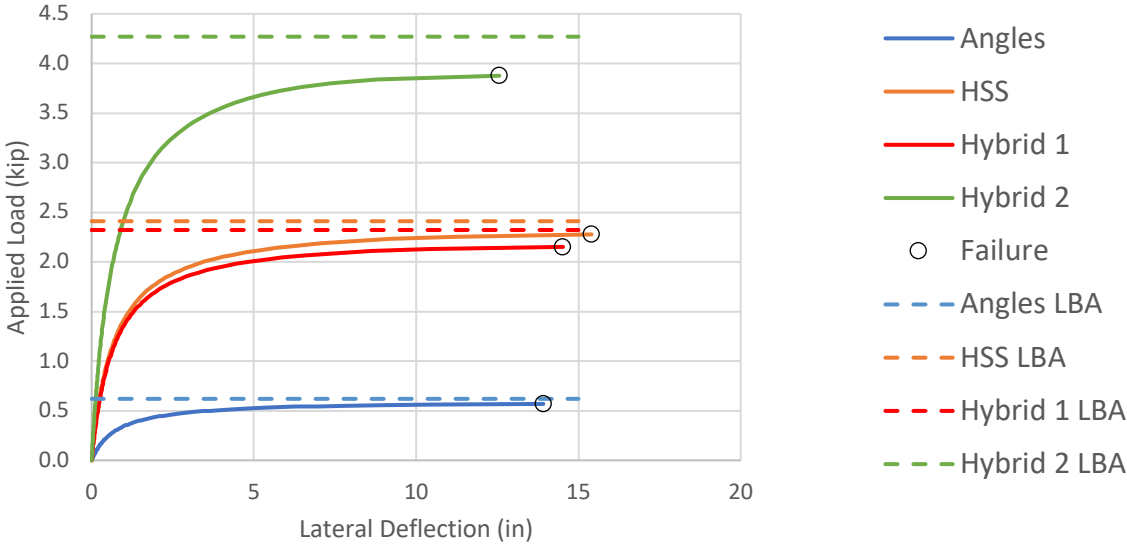


Figure 33. Point Load – GMNIA deflection including self-weight

4.2 DISTRIBUTED GRAVITY LOAD RESULTS

4.2.1 UNBRACED

Table 5 shows the unbraced distributed gravity load capacities for both the LBA and GMNIA analyses. Both analyses show the Angles design with the lowest capacity followed by the Hybrid 1 just below the HSS design, both with almost three times the capacity of the Angles design. The Hybrid 2 design again has the highest capacity of more than four and a half times the capacity of the Angles design. With exception of the Hybrid 2 design, all joists are impacted by the nonlinear and inelastic effects more significantly than in the point loading case. In this loading case, the Angles design is impacted slightly more than the Hybrid 1 and more than twice as much as the Hybrid 2. The HSS design is impacted slightly more than the Angles design which explains why

the capacity load ratio for the HSS decreases, but the other designs increase when taking into account nonlinear and inelastic behavior.

Table 5. Unbraced Distributed Gravity Load – Impact of nonlinear and inelastic behavior

	Failure Load in lbs/ft (Angles Capacity Load Ratio)			
	Angles	HSS	Hybrid 1	Hybrid 2
LBA	34 (1.00)	99 (2.91)	91 (2.68)	154 (4.51)
GMNIA	29 (1.00)	82 (2.85)	79 (2.72)	142 (4.91)
Capacity Decrease	15%	17%	14%	7%

Similar to the point load case, Table 6 shows that there is no decrease in capacity when running a GMNIA compared to a GNIA with. The decrease in capacity of the GMNIA from the LBA are again purely a result of the initial imperfection and shows that this elastic response is not dependent on the loading type, but rather dependent on the cross section and unbraced length. The perfectly elastic behavior can be confirmed in the same way as the point load case by noting that the GMNIA Deflections in Figure 34 and the GMNIA deflection curves in Figure 35 have their limit state capacities at the same deflection.

Table 6. Unbraced Distributed Gravity Load – Impact of steel yielding

	Limit State Load in lbs/ft (Angles Capacity Load Ratio)			
	Angles	HSS	Hybrid 1	Hybrid 2
GNIA	24 (1.00)	67 (2.81)	65 (2.74)	118 (4.96)
GMNIA	24 (1.00)	67 (2.81)	65 (2.74)	118 (4.96)
Capacity Decrease	0%	0%	0%	0%

All four joist designs, again, similar to the point load results, exhibit similar stiffness to each other, resulting in limit state capacities at approximately the same deflection as seen in Figure 34 and Figure 35. The limit state capacities follow a similar trend to the failure capacities with the Angles design at the limit state. The Angles design remains the joist with the lowest capacity

followed by the Hybrid 1 and HSS, which are just above three and a half times the capacity of the angles model. Meanwhile, the HSS design performs four and a half times the Angles design capacity.

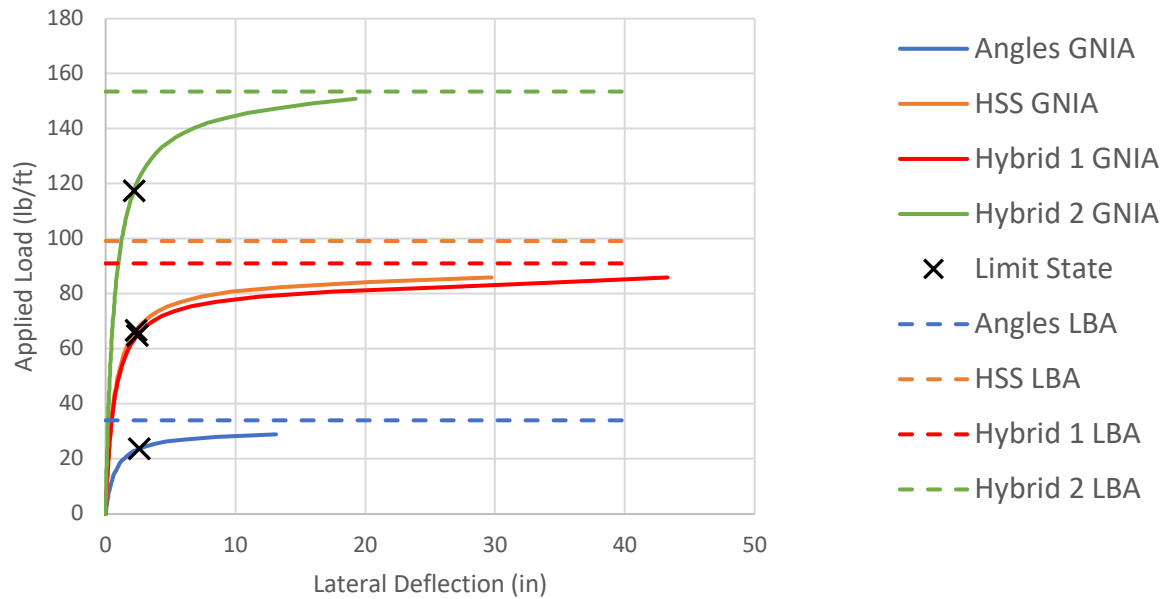


Figure 34. Unbraced Distributed Gravity Load – GNIA deflection

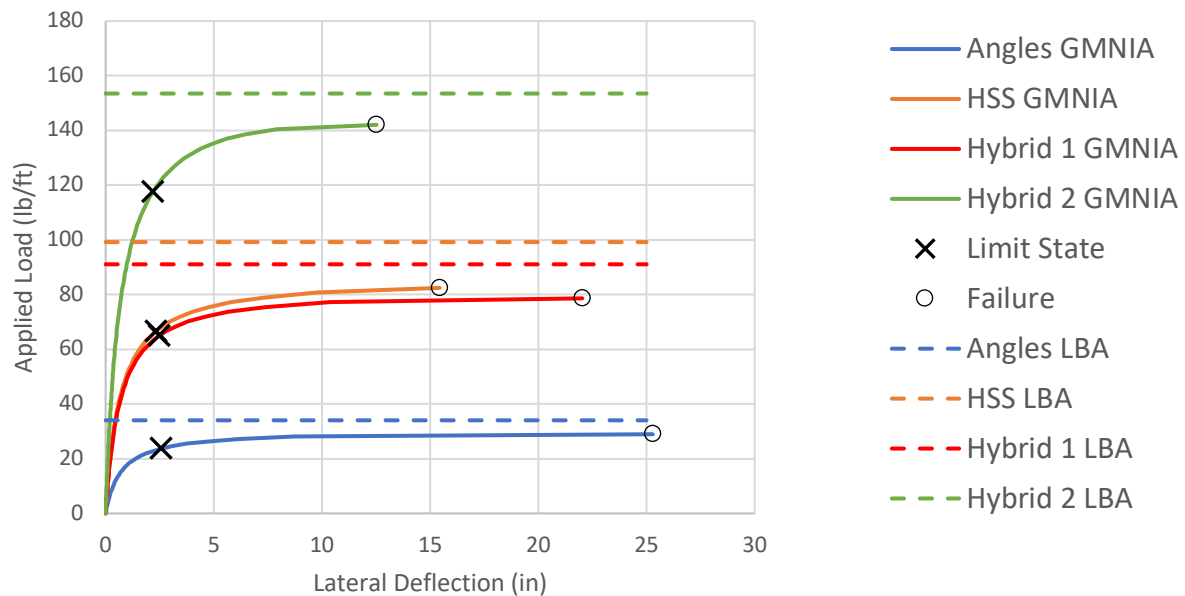


Figure 35. Unbraced Distributed Gravity Load – GMNIA deflection

The inclusion of self-weight affects each joist quite similarly to the point load case. The angles capacity is reduced by over 40 percent again while all the other joist design capacities are reduced by less than 20 percent as seen in Table 7. Just like in the point load case, the Hybrid 2 has the lowest impact from including self-weight because it has the highest unbraced load capacity.

Table 7. Unbraced Distributed Gravity Load – Impact of self-weight

	GMNIA Failure Load in lbs/ft (Angles Capacity Load Ratio)			
	Angles	HSS	Hybrid 1	Hybrid 2
Neglecting Self-Weight	29 (1.00)	82 (2.85)	79 (2.72)	142 (4.91)
Including Self-Weight	17 (1.00)	68 (4.05)	64 (3.77)	128 (7.60)
Capacity Decrease	42%	17%	19%	10%

The deflections at failure of these models are also impacted by the inclusion of self-weight as seen in Figure 36. The Angles design and the Hybrid 1 design have significantly higher deflections before adding self-weight while the HSS and Hybrid 2 have approximately the same deflection at failure after adding self-weight.

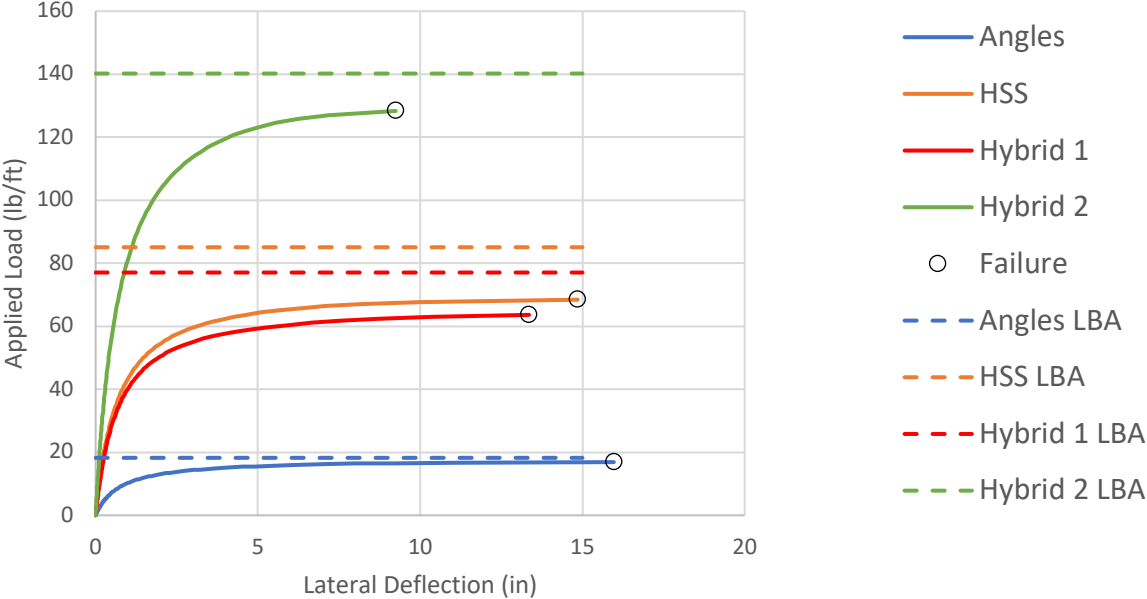


Figure 36. Unbraced Distributed Gravity Load – GMNIA deflection including self-weight

4.2.2 MID-SPAN BRACED

Table 8 shows that in the mid-span braced condition, the Hybrid 1 is impacted by the inelastic and nonlinear effects by almost twice as much as any of the other joist designs. Both analyses still agree on an order of capacity with the Angles design having the lowest capacity followed by the Hybrid 1 just below the HSS model, both with almost two times the capacity of the Angles model. The Hybrid 2 model has the highest capacity of more than three times the capacity of the angles model. While the mid-span braced loading condition shows the Angles joist as having the lowest capacity, the Angles capacity load ratio on all the other joists is decreasing. The HSS, Hybrid 1 and Hybrid 2 designs have their capacities scaled by a similar amount compared to the unbraced condition while the Angles capacity is scaled by a larger factor.

Table 8. Mid-span Braced Distributed Gravity Load – Impact of nonlinear and inelastic behavior

	Failure Load in lbs/ft (Angles Capacity Load Ratio)			
	Angles	HSS	Hybrid 1	Hybrid 2
LBA	111 (1.00)	192 (1.73)	186 (1.67)	352 (3.17)
GMNIA	93 (1.00)	170 (1.83)	132 (1.42)	295 (3.17)
Capacity Decrease	16%	11%	29%	16%

Now that the joists have a shorter unbraced length, the Hybrid models are starting to have yielding impact their capacities as seen in Table 9. It makes sense that these two joists are being impacted by yielding because the alterations made in the designs made the capacity of the chords significantly higher while the web members remained the same. The web members for the Hybrid 1 model were picked based on their cross-sectional area rather than their capacity and the web members for the Hybrid 2 were designed for lower capacity chords. This could force the web members to take more load than they may be designed for leading to partial yielding in the web

members. The GNIA analysis shows significantly more difference in the limit state capacity for the Hybrid 1 design than the Hybrid 2 design. If 13% of the 29% impact of nonlinear and inelastic behavior from Table 8 is a result of steel yielding as shown in Table 9, then the impact of just the initial imperfection is only 16% which is approximately the same impact as the other three joist designs. Under this mid-span braced loading case, only the HSS and Angles joists are slender enough to undergo pure elastic lateral-torsional buckling.

Table 9. Mid-span Braced Distributed Gravity Load – Impact of steel yielding

	Limit State Load in lbs/ft (Angles Capacity Load Ratio)			
	Angles	HSS	Hybrid 1	Hybrid 2
GNIA	81 (1.00)	146 (1.80)	149 (1.85)	270 (3.35)
GMNIA	81 (1.00)	146 (1.80)	129 (1.60)	267 (3.30)
Capacity Decrease	0%	0%	13%	1%

The limit state results are not as consistent as they were with the unbraced case. The Hybrid 1 shows a higher capacity than the HSS in the GNIA study, but has the largest impact of steel yielding and therefore has a lower capacity than the HSS with the GMNIA study. It is important to note that the Hybrid 1 design is much less stiff than any of the other joist designs and undergoes over 4 times the deflection of any other joist at the limit state capacity as seen in Figure 37 and Figure 38.

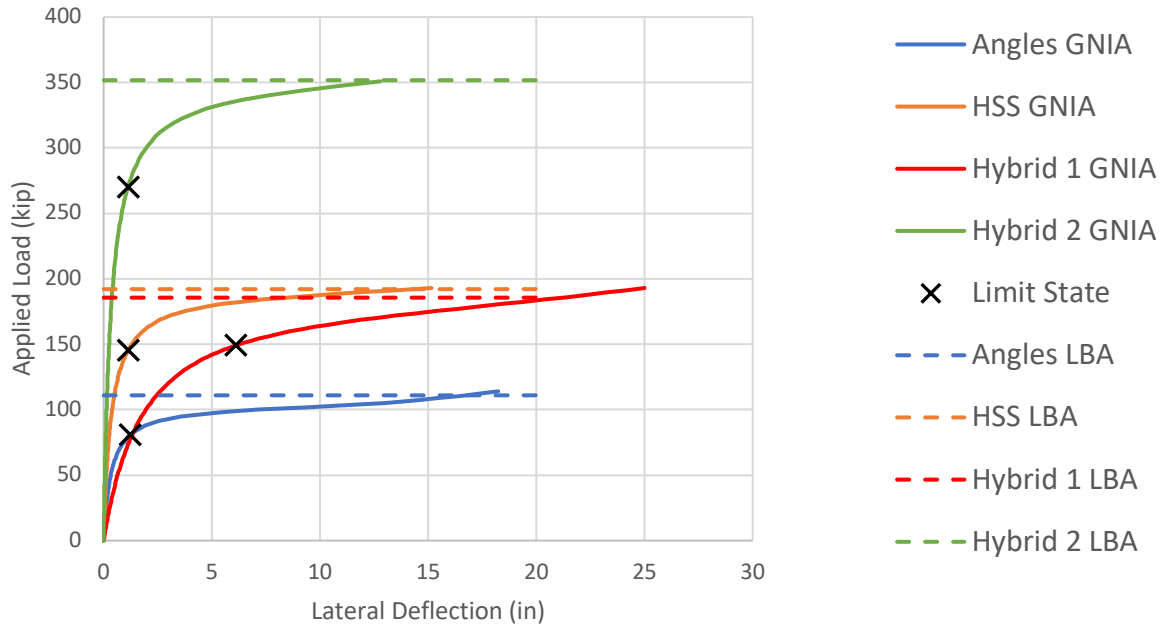


Figure 37. Mid-span Braced Distributed Gravity Load – GNIA deflection

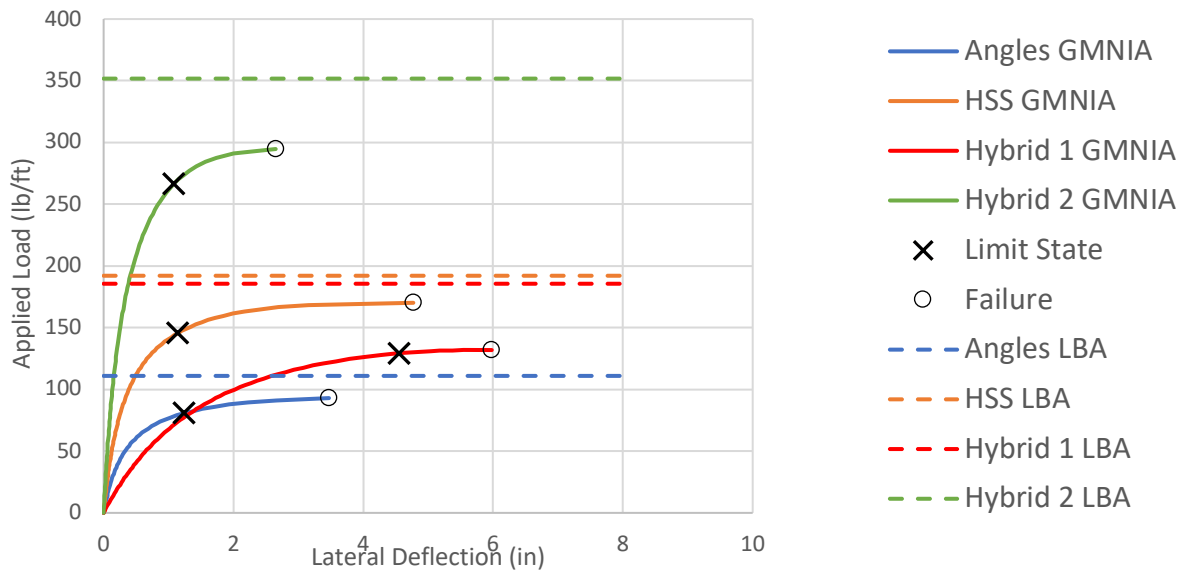


Figure 38. Mid-span Braced Distributed Gravity Load – GMNIA deflection

Similar to the unbraced case, self-weight has the largest impacts on the Angles designs as seen in Table 10. The HSS and Hybrid 1 designs have about a ten percent decrease in capacity when including self-weight while the Hybrid 2 design has a slightly smaller decrease in capacity of five

percent. These percent differences are closer together because the variance in joist capacity is closer together.

Table 10. Mid-span Braced Distributed Gravity Load – Impact of self-weight

	GMNIA Failure Load in lbs/ft (Angles Capacity Load Ratio)			
	Angles	HSS	Hybrid 1	Hybrid 2
Neglecting Self-Weight	93 (1.00)	170 (1.83)	132 (1.42)	295 (3.17)
Including Self-Weight	80 (1.00)	156 (1.94)	117 (1.46)	280 (3.48)
Capacity Decrease	14%	9%	11%	5%

The deflections at failure of these designs are also impacted by the inclusion of self-weight as seen in Figure 39. The Angles and HSS designs have higher deflections than before adding self-weight showing an increase in deflection at failure while the Hybrid 1 and Hybrid 2 models have lower deflections showing a decrease in deflection at failure.

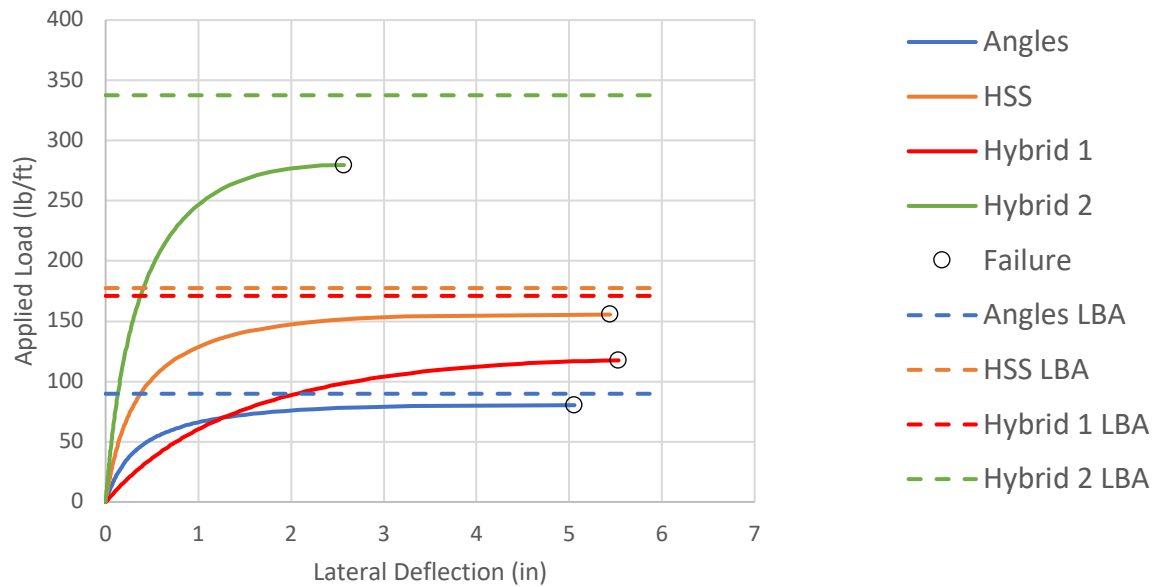


Figure 39. Mid-span Braced Distributed Gravity Load – GMNIA deflection including self-weight

**Table 11. Quarter Braced Distributed Gravity Load –
Impact of nonlinear and inelastic behavior**

	Failure Load in lbs/ft (Angles Capacity Load Ratio)			
	Angles	HSS	Hybrid 1	Hybrid 2
LBA	356 (1.00)	288 (0.81)	280 (0.79)	858 (2.41)
GMNIA	288 (1.00)	240 (0.84)	201 (0.70)	504 (1.75)
Capacity Decrease	19%	17%	28%	41%

With the quarter braced condition, all four designs have some impact from yielding. The decreases in their capacities can be seen in Table 12. Just like in the mid-span braced condition, both the Hybrid 1 and Hybrid 2 designs are impacted more than the Angles or HSS designs when accounting for the steel yielding. If the impact of steel yielding is subtracted from the impacts of nonlinear and inelastic behavior, the impacts of the initial imperfections are all approximately the same, around a 15 to 20 percent decrease in capacity.

Table 12. Quarter Braced Distributed Gravity Load – Impact of steel yielding

	Limit State Load in lbs/ft (Angles Capacity Load Ratio)			
	Angles	HSS	Hybrid 1	Hybrid 2
GNIA	274 (1.00)	219 (0.80)	207 (0.76)	649 (2.37)
GMNIA	263 (1.00)	216 (0.82)	186 (0.71)	482 (1.83)
Capacity Decrease	4%	2%	10%	26%

The limit state results are more consistent than they were with the mid-span braced case. The Hybrid 1 design is still less stiff than any of the other joist design, but in the quarter braced case, only undergoes 1.5 times the deflection of any other joist at the limit state capacity as seen in Figure 41 and Figure 42. When looking at the GMNIA, the Hybrid 2 is almost twice as stiff as a result of the impact of self-weight on the joist.

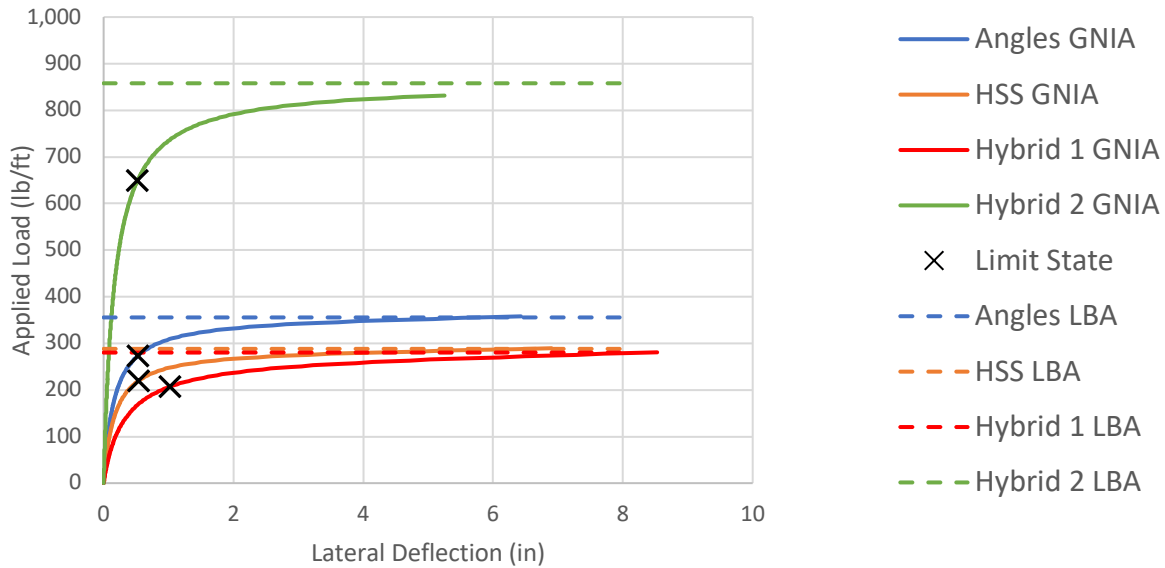


Figure 41. Quarter Braced Distributed Gravity Load – GNIA deflection

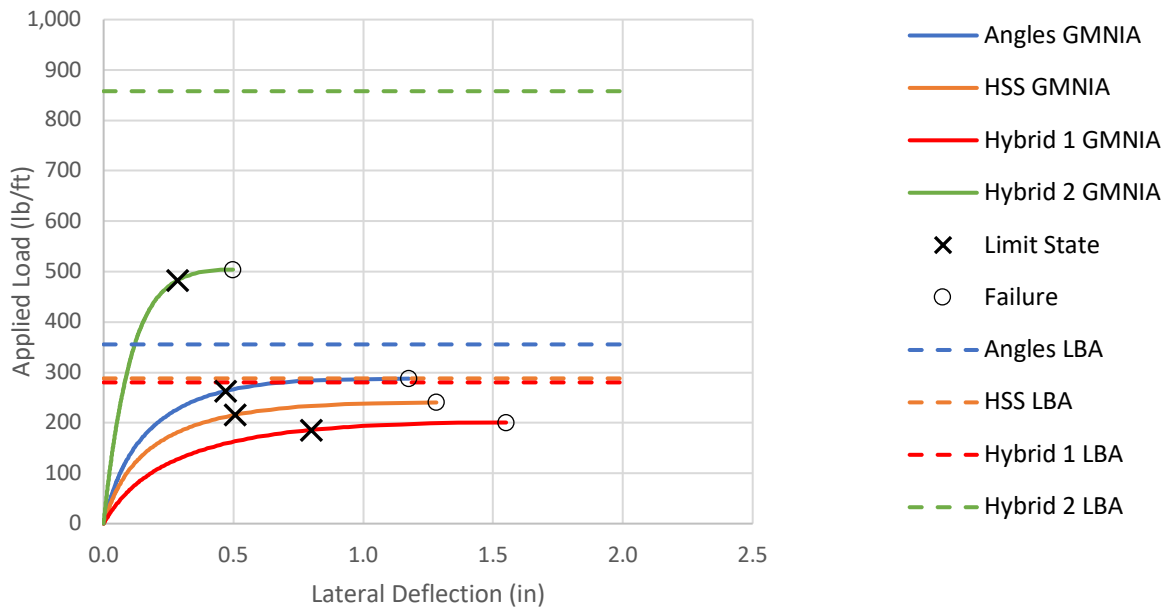


Figure 42. Quarter Braced Distributed Gravity Load – GMNIA deflection

As seen in Table 13, self-weight has a much smaller impact on the capacities of all the joint designs with around a five percent reduction in capacity. Just like in the other loading cases self-weight impacts the Hybrid 2 the least because it has the highest capacity and, in this case, impacts the Hybrid 1 the most because it has the lowest capacity.

Table 13. Quarter Braced Distributed Gravity Load – Impact of self-weight

	GMNIA Failure Load in lbs/ft (Angles Capacity Load Ratio)			
	Angles	HSS	Hybrid 1	Hybrid 2
Neglecting Self-Weight	288 (1.00)	240 (0.84)	201 (0.70)	504 (1.75)
Including Self-Weight	273 (1.00)	225 (0.82)	186 (0.68)	490 (1.79)
Capacity Decrease	5%	6%	7%	3%

The deflections at failure of these designs are also impacted by the inclusion of self-weight as seen in Figure 43. The Angles and HSS designs have slightly lower deflections than before adding self-weight while the Hybrid 2 has about half of the deflection at failure after including self-weight. The Hybrid 1 had the same deflection at failure before and after considering self-weight.

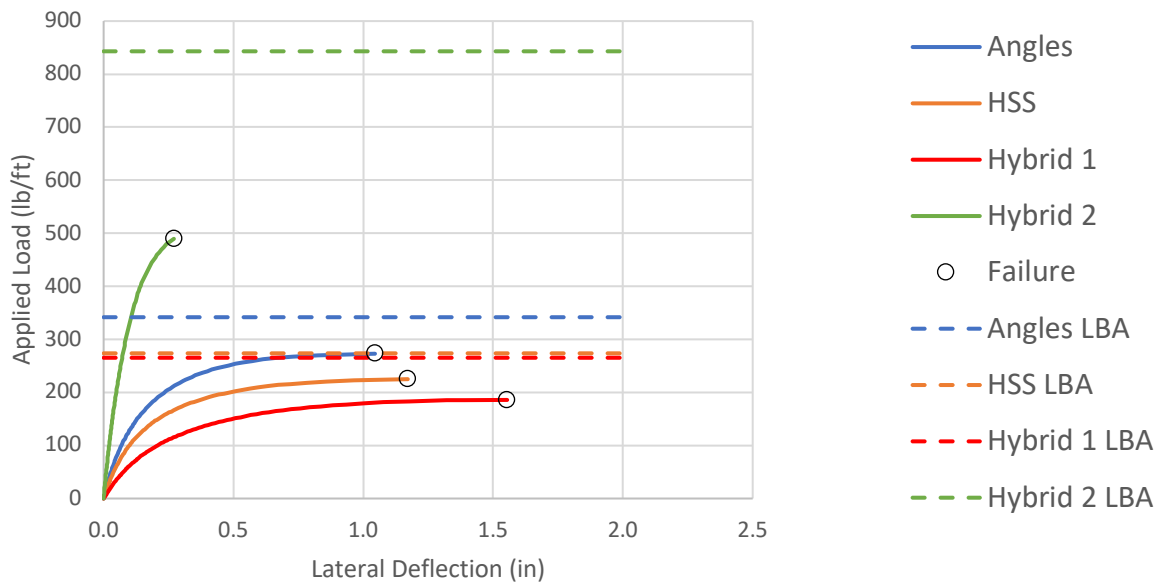


Figure 43. Quarter Braced Distributed Gravity Load – GMNIA deflection with self-weight

4.2.4 IMPACT OF UNBRACED LENGTH

While each distributed gravity load study considers a specific unbraced length, it is interesting to compare how the capacities of each joist are impacted by a change to the unbraced length. Figure 44 shows a comparison of the predicted joist capacities from Equation 1 in Chapter 2 of this thesis to the GMNIA results not including self-weight. While each predicted capacity is relatively close to the actual capacities determined from the GMNIA results, the GMNIA for the Angles design is providing higher values than predicted while the other three models are providing significantly lower capacities compared to the predicted capacities from Equation 1. This is important to recognize because it shows that the capacity approximations from Equation 1 appear to show the joists with HSS chords as having much higher relative capacities, when in reality their capacities overlap as the unbraced length changes.

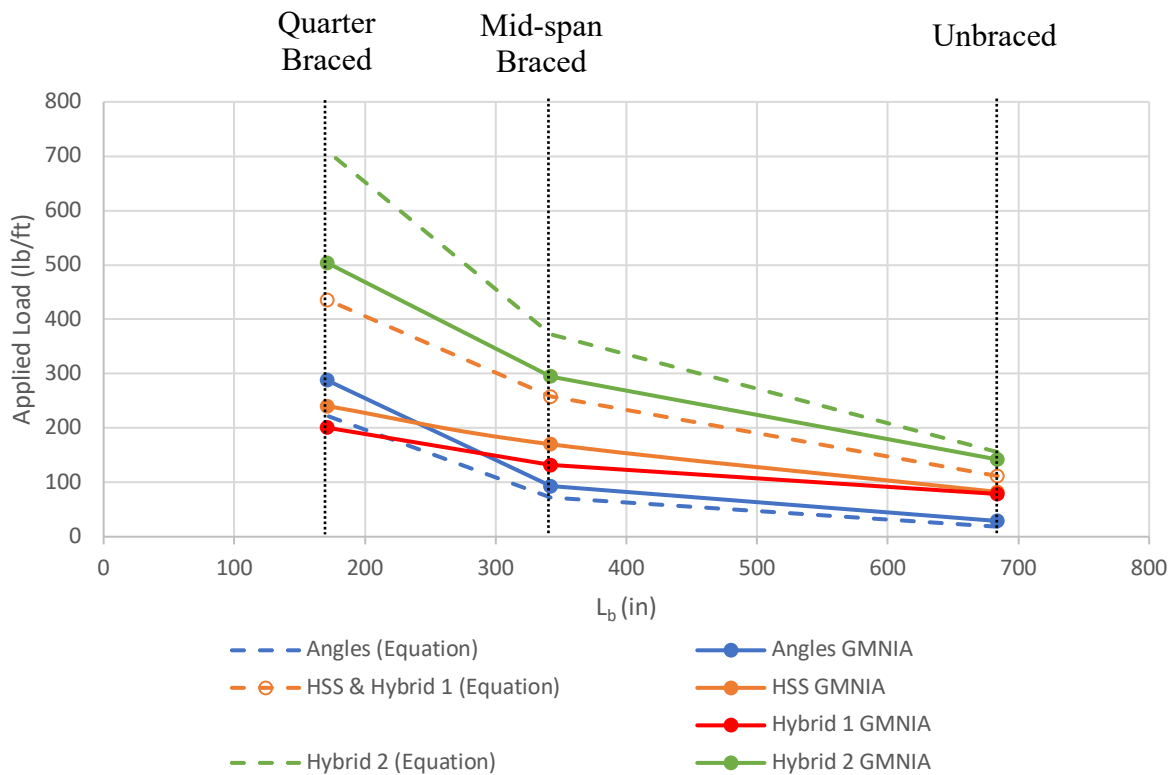


Figure 44. GMNIA capacities compared with anticipated results

When comparing the distributed gravity load GMNIA results including self-weight for the various unbraced lengths, the trends of each design remain the same, just with lower capacities as seen in Figure 45. One important note is that the Angle and Hybrid 2 designs both included vertical web members and show a greater rate of increase in capacity as the unbraced length decreases compared to the other designs which suggests that the web members have a more significant impact than initial assumed.

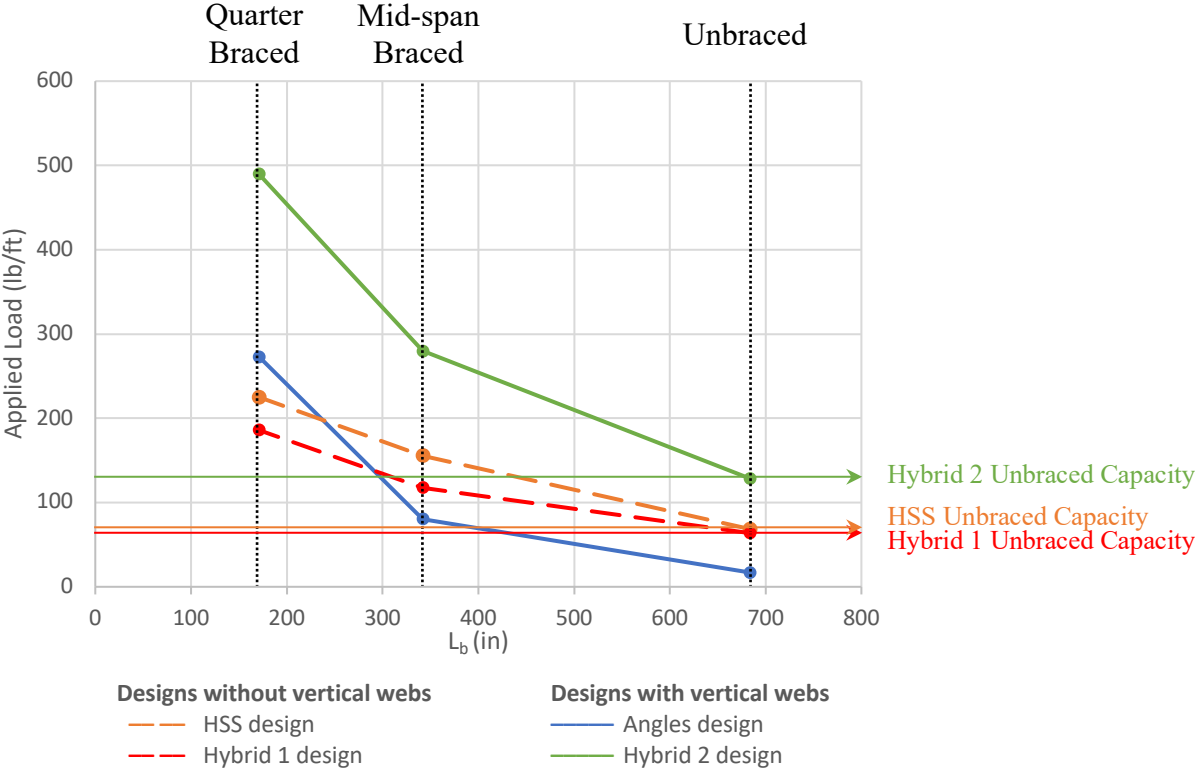


Figure 45. GMNIA capacity as a function of unbraced length with self-weight

Although the HSS and Hybrid 1 designs outperform the Angles design in the unbraced and mid-span braced conditions, the mid-span braced angles joist barely outperforms the unbraced HSS design and Hybrid 1 design capacities as seen in Figure 45. The unbraced Hybrid 2, however, is able to outperform the mid-span braced Angles design, but not the quarter braced

angles capacity. This suggests not all bridging can be removed to achieve the quarter braced Angles capacity, but possibly that the amount of bridging can be reduced.

4.3 UPLIFT RESULTS

The uplift analysis, while important, was not evaluated as comprehensively as the distributed gravity load analysis for this study. Only an LBA study was performed, but the impact of including self-weight was still analyzed. Unlike the previous loading cases, self-weight is counteracting the applied loads and therefore increases the uplift capacities of the joists. The Hybrid 2 was not included in this study due to its creation later into the study. As stated previously, all uplift cases have uplift bridging on the bottom edges of the chords, no matter how the joist is braced.

4.3.1 UNBRACED

For the unbraced uplift case, the HSS and Hybrid 1 provide equivalent uplift capacities of almost three times that of the angles as seen in Table 14. Similar to the distributed gravity load results, self-weight has the more significant percentage impact on the Angles design. The Hybrid 1 and HSS provide the same capacities of between two and a half and three times larger than the Angles design.

Table 14. Unbraced Uplift - Impact of self-weight

	LBA Failure Load in lbs/ft (Angles Capacity Load Ratio)		
	Angles	HSS	Hybrid 1
Neglecting Self-Weight	54 (1.00)	158 (2.94)	158 (2.94)
Including Self-Weight	70 (1.00)	174 (2.49)	174 (2.49)
Capacity Increase	30%	10%	10%

4.3.2 MID-SPAN BRACED

For the mid-span braced uplift case the HSS and Hybrid 1 provide similar uplift capacities just above two times that of the Angles as seen in Table 15. Just like in the unbraced case, the inclusion of self-weight has the highest percentage benefit to the Angles design. The HSS design has the highest capacity of around twice that of the Angles design with the Hybrid 1 design having just slightly below the HSS capacity.

Table 15. Mid-span Braced Uplift - Impact of self-weight

	LBA Failure Load in lbs/ft (Angles Capacity Load Ratio)		
	Angles	HSS	Hybrid 1
Neglecting Self-Weight	115 (1.00)	240 (2.09)	236 (2.05)
Including Self-Weight	130 (1.00)	255 (1.96)	251 (1.93)
Capacity Increase	13%	6%	7%

4.3.3 QUARTER BRACED

For the quarter braced uplift case the HSS and Hybrid 1 again provide similar uplift capacities just above 1.3 times that of the Angles as seen in Table 16. The HSS and Hybrid 1 have capacities of just over 30 percent that of the Angles design capacity.

Table 16. Quarter Braced Uplift - Impact of self-weight

	LBA Failure Load in lbs/ft (Angles Capacity Load Ratio)		
	Angles	HSS	Hybrid 1
Without Weight	265 (1.00)	355 (1.34)	347 (1.31)
With Weight	280 (1.00)	370 (1.32)	363 (1.30)
Capacity Increase	6%	4%	4%

4.3.4 IMPACT OF UNBRACED LENGTH

The uplift GMNIA capacities can be compared as a function of the unbraced length as seen in Figure 46. The Hybrid 1 and HSS outperform the Angles design with a similar capacity in all unbraced lengths. While the angle increase in capacity as the unbraced length decreases faster than the HSS and Hybrid 1 designs, it does not increase significantly enough to outperform the HSS and Hybrid 1.

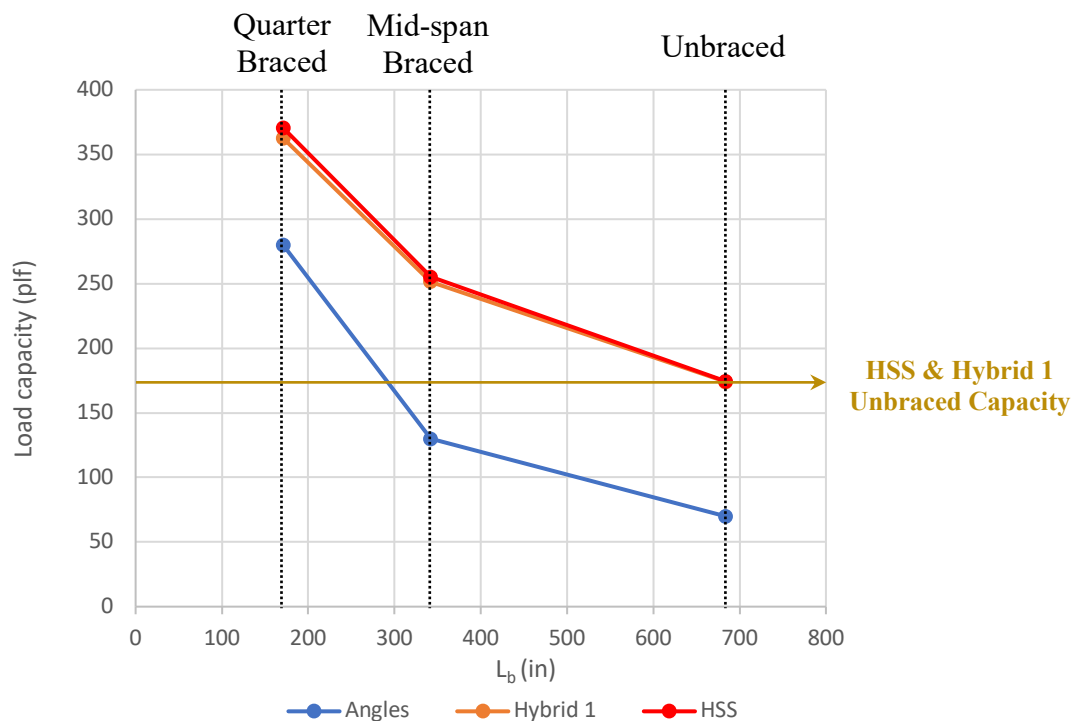


Figure 46. LBA uplift capacity as a function of unbraced length with self-weight

Unlike with the gravity loading, the unbraced HSS and Hybrid 1 designs outperform the Angles design in the mid-span braced condition as seen in Figure 46. The unbraced HSS and Hybrid 1 designs are still not able to outperform the quarter braced Angles design capacity. This again suggests not all bridging can be removed to achieve the quarter braced Angles capacity, but possibly that the amount of bridging can be reduced.

CHAPTER 5: CONCLUSIONS

5.1 SUMMARY OF RESULTS

Based on the analyses performed, the use of HSS in the chords is able to substantially increase the strength of a joist, and can potentially reduce the amount of bridging needed, but not fully eliminate it. While HSS members in the chords provide high load capacities for the initial erection of a joist and for distributed loads over large unbraced lengths, the unbraced capacity does not exceed the capacity of the quarter braced Angles design. The main benefit of using the HSS sections in the chords is the increased capacity and therefore safety of the initial joist erection.

The HSS design slightly outperformed the Hybrid 1 design, but the difference was negligible in all analyses. Having angle webs attached to the sides of the chords allows for less complex fabrication and likely, a more economical design without compromising the strength of the joist.

Using HSS for the chords and angles for the webs in the Hybrid 1 and Hybrid 2 designs provided overall high capacities supporting the initial assumption that the chords control the joist capacity. The Hybrid 1 had some problems with low stiffness at smaller unbraced lengths, but this can likely be resolved by using double angles at the end diagonals. Attaching end members on only one side of the chords causes the high loads being transferred from the bottom chord to the joist support, to also impose an eccentricity on the end diagonals lowering the stiffness of the entire joist. The Hybrid 2 had problems with web members yielding, but this should be able to be resolved by redesigning the web members for that joist.

Overall, HSS in the chords can provide stronger joists for more stability during erection and throughout loading over the lifespan of the joist. Based on this 32LH06 joist design and looking at just the point load case, a joist with a single HSS member in each chord can support a load of

four times that of an equivalent joist with double angle chords. A joist with double HSS chords is able to provide around seven times the capacity of an equivalent joist with a double angle chord. By performing further studies to adjust the joist designs to become even more efficient with their use of HSS members in the chords, these capacity ratios will only increase.

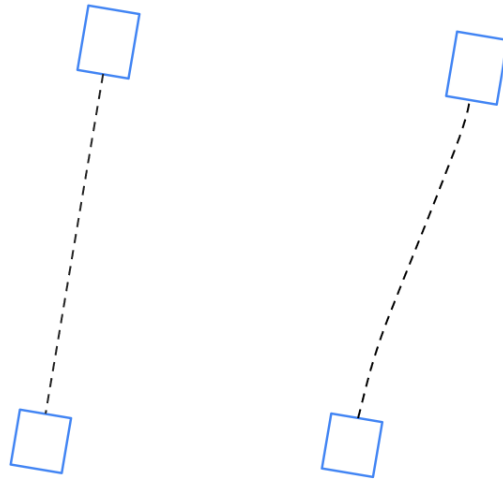
5.2 FURTHER STUDIES

5.2.1 FURTHER ANALYSIS OF THE HYBRID 2 MODEL

Based on the analyses performed in this study, the Hybrid 2 model appears to outperform the other models significantly, but it is important to consider that this model was a later addition to this study and was not made into a mixed or shell model. This means the model assumed that the chords are each a cross-section rather than two HSS sections running parallel to each other. While this simplification was used for the double angles, the double tubes have thin sides that could result in local buckling along the cross section. A mixed element or shell model is required to check if local buckling in the chords is problematic.

5.2.2 INCREASE WEB STIFFNESS

When comparing the single dimension line model and predicted results to the other models, there is a large inconsistency in the results. Their inconsistency may be a result of the assumption that there is no deformation in the cross-section of the joist (Figure 47) and that the chords remain in the same position relative to one another at any location. A study on the impacts of increasing the overall web stiffness by adding additional web members or altering the web cross-sections would help inform how to better design webs to support the full capacities of HSS chords.



a. No web deformation b. Some web deformation

Figure 47. Defection of the joist cross-section

REFERENCES

- AISC (2016). *Specification for structural steel buildings*. American Institute of Steel Construction (AISC), Steel Construction Manual, 15th ed.
- Armbrust, S. (2020) *32TLH06 Joist Design*. Xbow, LLC.
- Cole, D. (2018, October 31). *Work in progress: SVUSD bond projects continue apace*. Herald/Review Media. https://www.myheraldreview.com/news/business/work-in-progress-svUSD-bond-projects-continue-apace/article_d7a56d12-dceb-11e8-aae3-9f446695ca4a.html.
- Schwarz, J.E. (2002) *Stability of Unbraced steel Joists Subject to Mid-span Loading Phase II L2_32LH06 Joist Design (p. 95)*.
- SkyCiv (2021). *Section Builder Software* [Computer software]. Retrieved from <https://platform.skyciv.com/section-builder>.
- Steel Erectors Association of America (SEAA). (2020, October 12). *Open web steel joist safety*. <https://www.seaa.net/news/open-web-steel-joist-safety>.
- STRAND7 (2021) *Finite Element Analysis Software* [Computer software]. (2021). Retrieved from <https://www.strand7.com/>.
- U.S. Patent no. US 9,765,520 B2, Tubular Joist Structures and Assemblies and Methods of Using, September 19, 2017, Scott F. Armbrust and Scott A. Armbrust.
- U.S. Patent no. US 10,072,416 B2, Tubular Joist Structures and Assemblies and Methods of Using, September 11, 2019, Scott F. Armbrust and Scott A. Armbrust.

Ziemian, R.D., Liu, S.W., and McGuire, W. (2020) *MASTAN2* - v5.1 [Computer software].

Retrieved from <http://www.mastan2.com/>.

APPENDIX A: MODELS AND PROPERTIES

A-1 ANGLES DESIGN

L2_32LH06

PROPERTIES:

SPAN = 57'-0"

TOP CORD (2) = 2.5" x 2.5" x 0.212" w/ 1" GAP

BOTTOM CORD (2) = 2.0" x 2.0" x 0.216" w/ 1" GAP

W2 = 1.5" x 1.5" x .109 DOUBLE ANGLE

W3 = 2.0" x 2.0" x 0.187" CRIMPED

W4 = 1.25" x 1.25" x 0.109" CRIMPED

W5 = 1.75" x 1.75" x 0.155" CRIMPED

W6 = 1.0" x 1.0" x 0.109" STRAIGHT

W7 = 1.5" x 1.5" x 0.155" CRIMPED

W8 = 1.0" x 1.0" x 0.109" STRAIGHT

W9 = 1.5" x 1.5" x 0.155" CRIMPED

W10 = 1.0" x 1.0" x 0.109" STRAIGHT

W11 = 1.5" x 1.5" x 0.155" CRIMPED

V1 = 1.0" x 1.0" x 0.109" STRAIGHT

V2 = 1.0" x 1.0" x 0.109" STRAIGHT

WEIGHT = ? lb

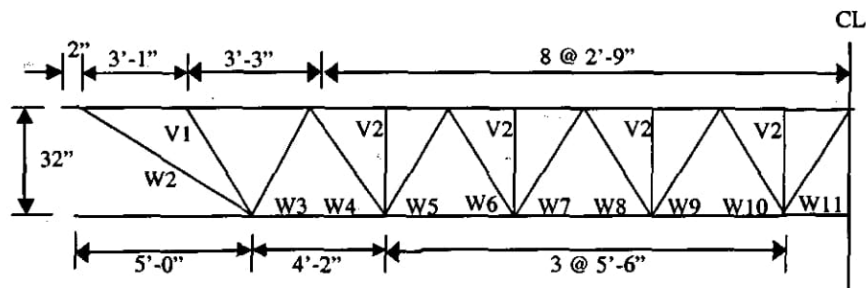


Figure 48. Geometric Properties of the Angles design (Schwarz, 2002)

A-2 HSS DESIGN

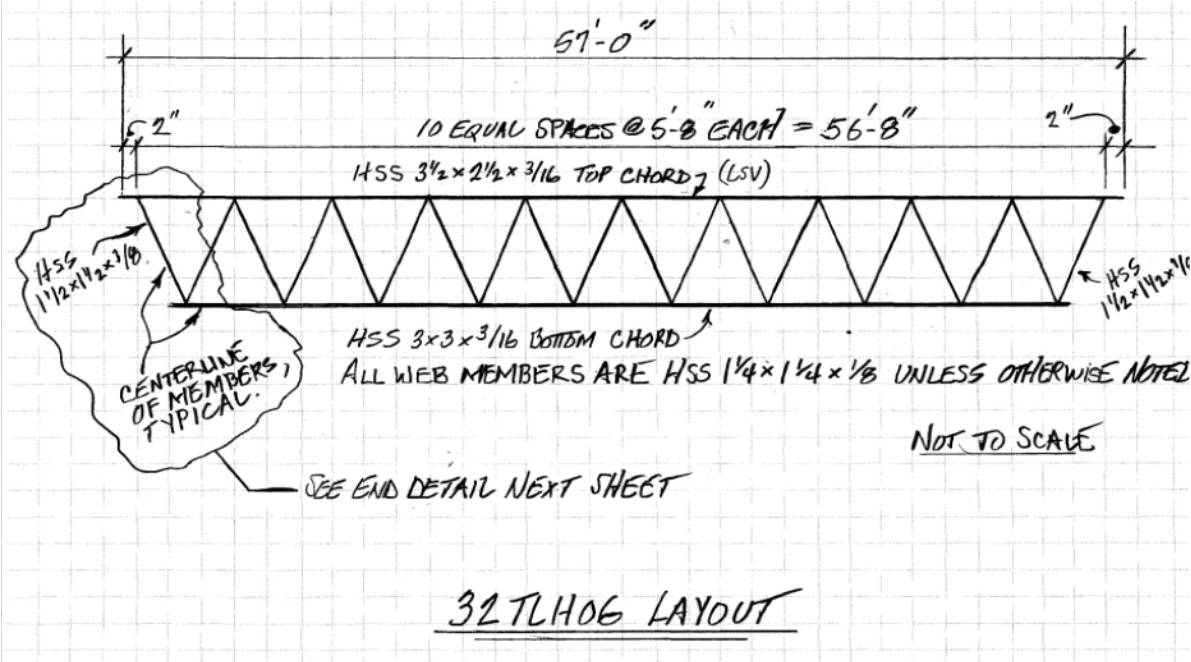


Figure 49. Geometric Properties of the HSS design (Armbrust, 2020)

A-3 HYBRID 1 DESIGN

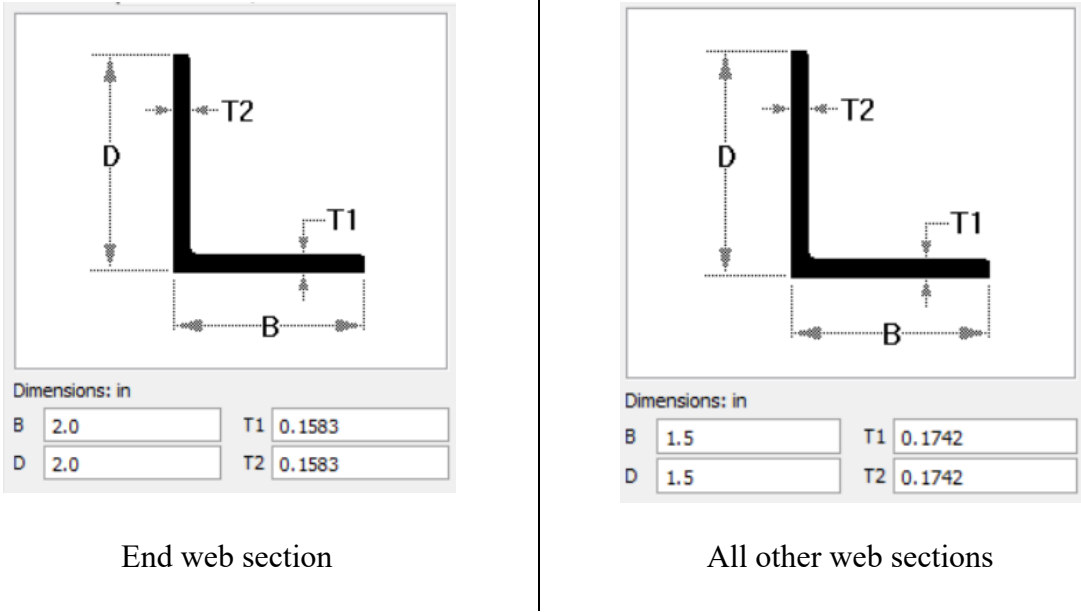
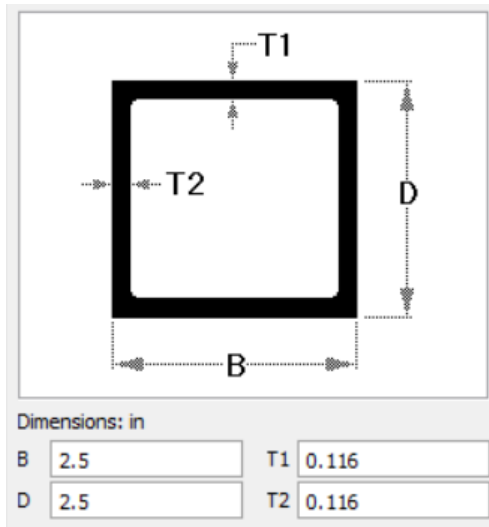
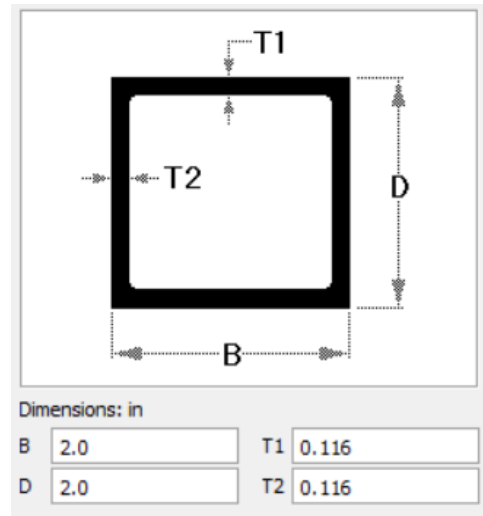


Figure 50. Web member changes to the HSS design for the Hybrid 1 design

A-4 HYBRID 2 DESIGN



Top Chord dimensions for 1 of 2 identical
double HSS sections spaced @ 1"



Bottom Chord dimensions for 1 of 2 identical
double HSS sections spaced @ 1"

Figure 51. Chord member changes to the Angles design for the Hybrid 2 design

APPENDIX B: FINITE ELEMENT MODELS

B-1 LINE ELEMENT MODELS

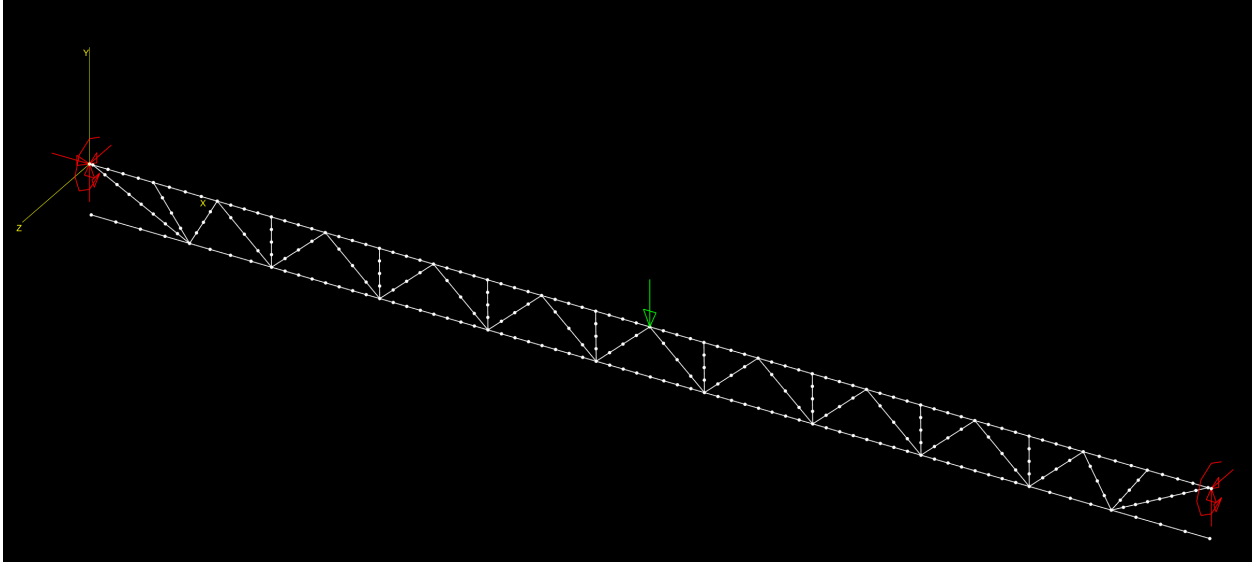


Figure 52. MASTAN2 line element model for the Angles design

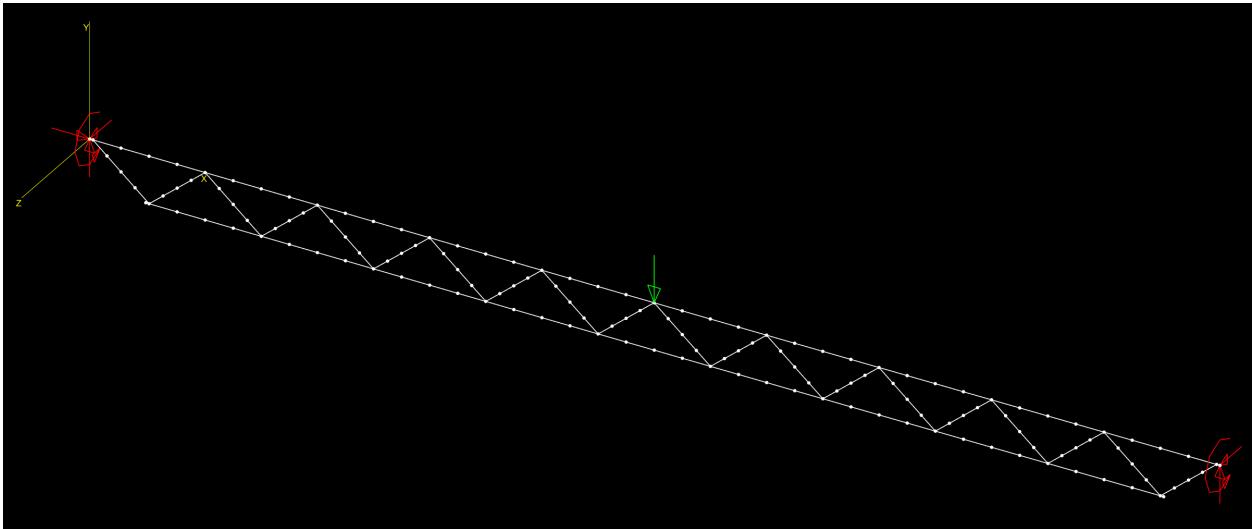


Figure 53. MASTAN2 line element model for the HSS design

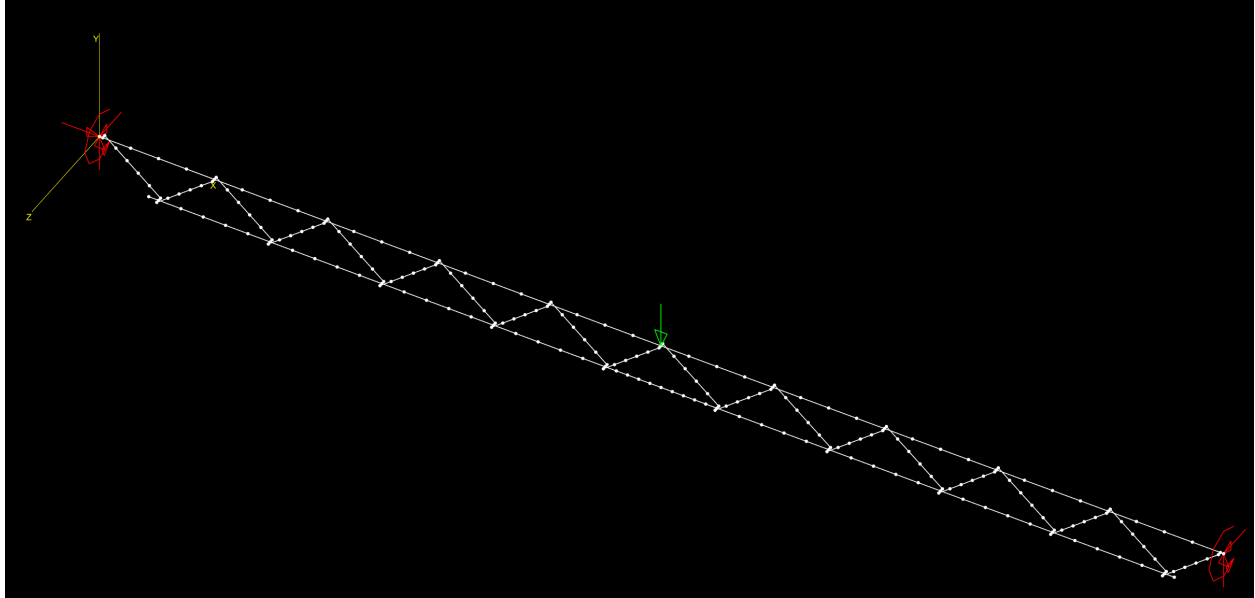


Figure 54. MASTAN2 line element model for the Hybrid 1 design

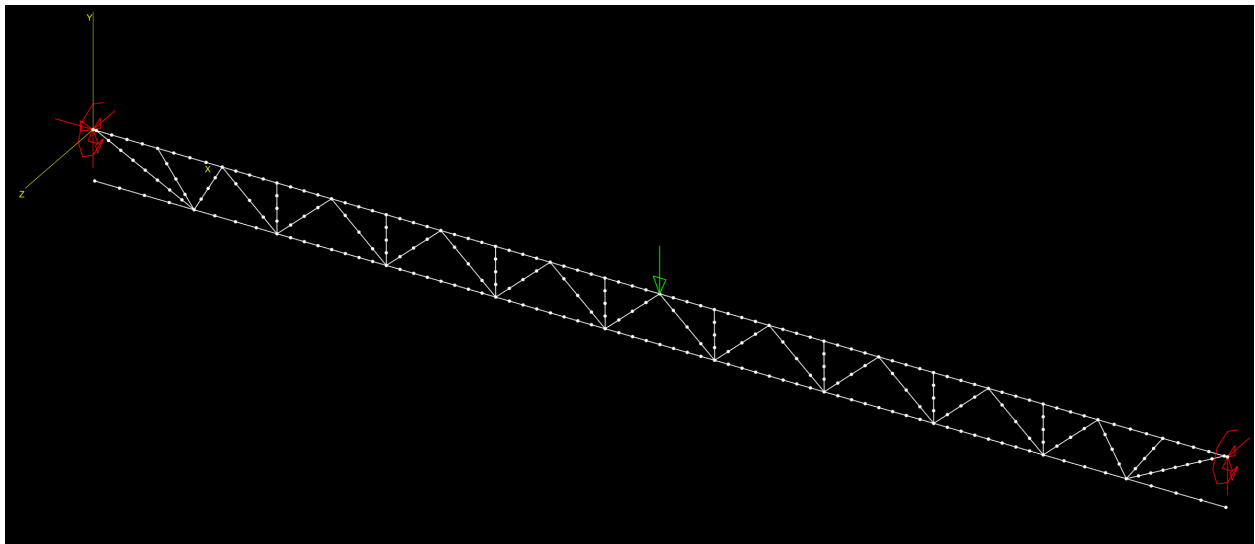


Figure 55. MASTAN2 line element model for the Hybrid 2 design

B-2 MIXED ELEMENT MODELS

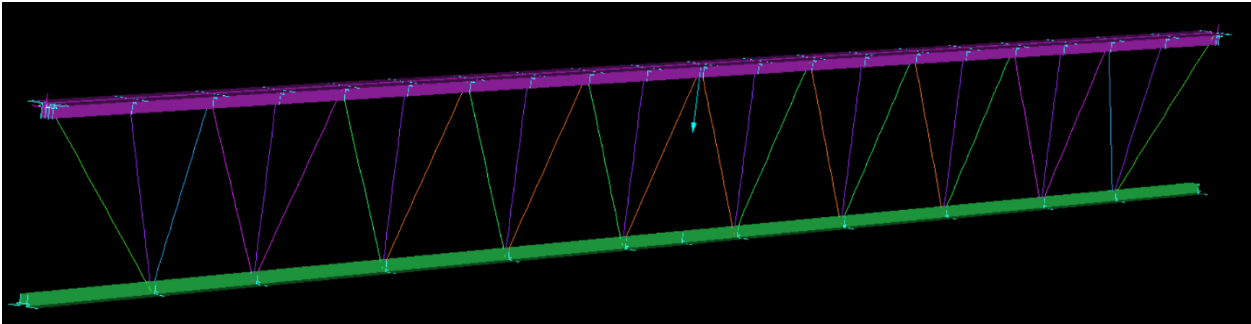


Figure 56. STRAND7 mixed element model for the Angles design

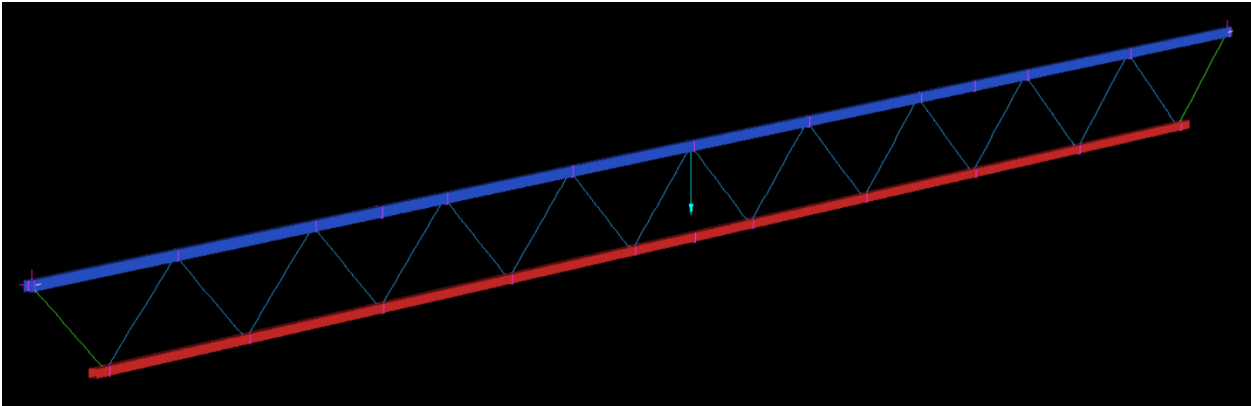


Figure 57. STRAND7 mixed element model for the HSS design

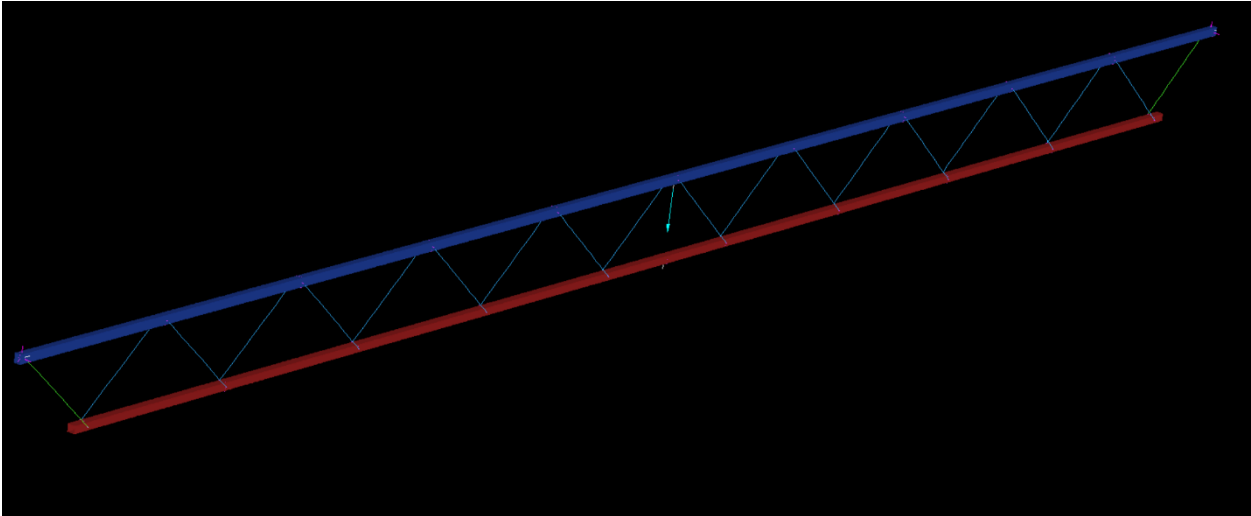


Figure 58. STRAND7 mixed element model for the Hybrid 1 design

B-3 SHELL ELEMENT MODELS

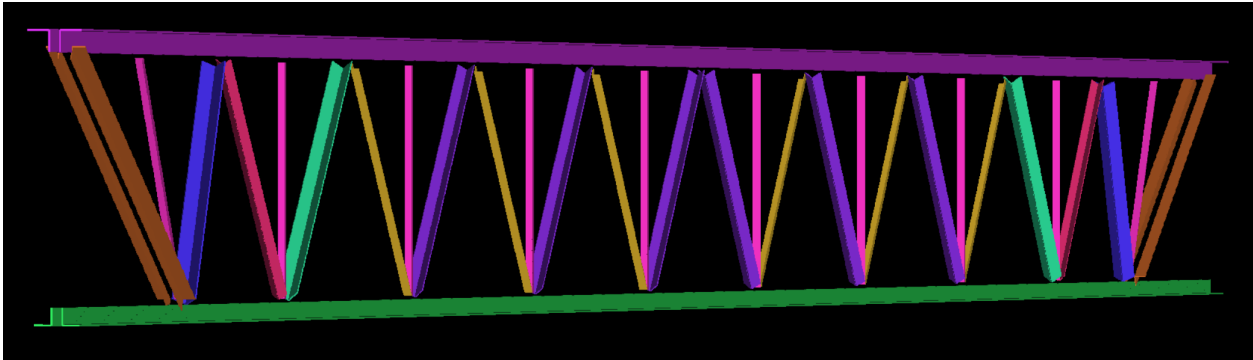


Figure 59. STRAND7 shell element model for the Angles design

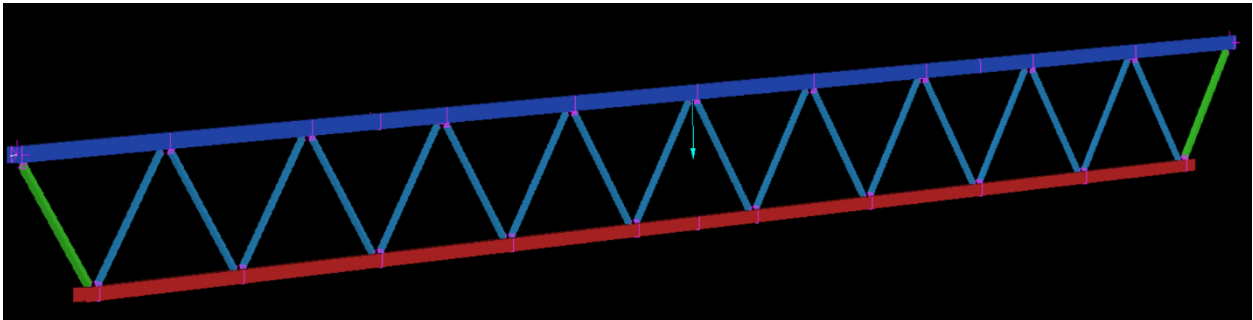


Figure 60. STRAND7 shell element model for the HSS design

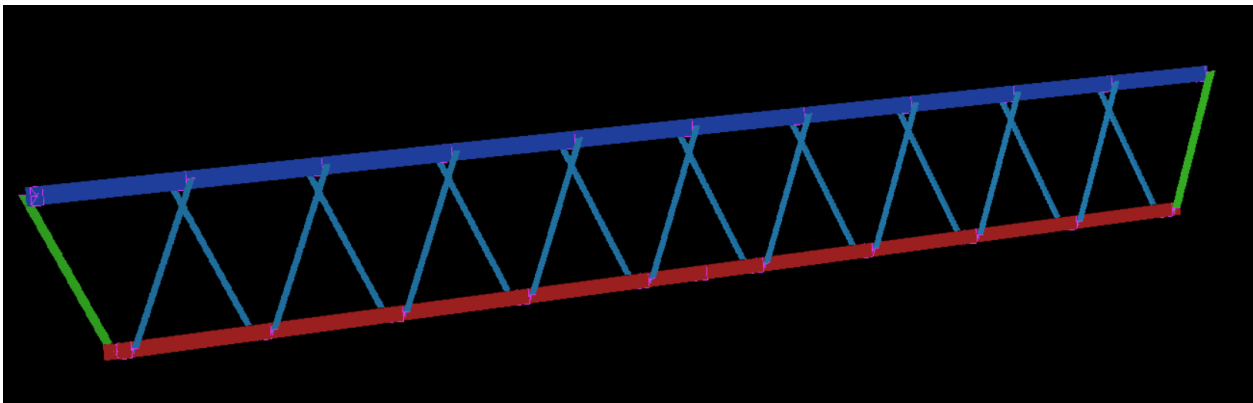


Figure 61. STRAND7 shell element model for the Hybrid 1 design